REVIEW ARTICLE

The (p,n) reaction and the nucleon-nucleon force

Rep. Prog. Phys. **50** (1987) 607-654. Printed in the UK

The (p, n) reaction and the nucleon–nucleon force

G F Bertsch† and H Esbensen‡

† Cyclotron Laboratory and Department of Physics and Astronomy, Michigan State University, East Lansing, MI 48824, USA
‡ Physics Division, Argonne National Laboratory, Argonne, IL 60439, USA

Abstract

The (p, n) charge exchange reaction is a powerful tool of nuclear structure physics, with spectroscopic characteristics that are closely related to the free interaction between nucleons. At proton energies in the range of 150–500 MeV, the interaction probes the spin dynamics in the charge exchange process and is particularly sensitive to nuclear pionic fields. At low energies, say less than 50 MeV bombarding energy, the reaction also probes the isovector density. An outstanding success of the reaction as a structural probe is the elucidation of the Gamow–Teller strength function in the nuclear excitation spectrum. However, the total strength found falls short of sum rule predictions by about 40%. Explanations of this quenching have been advanced along two lines, based on subnuclear degrees of freedom or on configuration mixing into high continuum states. Detailed theoretical arguments support the importance of configuration mixing. The subnuclear degrees of freedom may be comparable, but a decisive test is lacking.

This review was received in May 1986.

0034-4885/87/060607+49$09.00

Contents

1. Introduction

Inelastic scattering of nucleons from nuclei has provided much information about nuclear structure. The reaction has large cross sections, and delicate studies are possible, varying the energy and momentum transfer to the target independently. The nucleon interaction has several couplings that allow many different kinds of excitations to be investigated. One important interaction of fundamental interest is the pion coupling to nuclear states. The pion itself is not the best probe, however, because the kinematics of the absorption or emission process limits which states can be studied. Inelastic nucleon scattering can probe all states at low excitation, and the part mediated by the virtual pion field can be emphasised. Pionic interactions are important in the charge exchange reaction because charged pions can be exchanged between the projectile nucleon and the target, while much of the remaining interaction at small momentum transfers is not mediated by charged mesons. Other probes that interact via the electroweak field are more precise because the interaction is a well understood perturbation. However, many aspects of nuclear structure are not accessible to these probes, for reasons of restricted couplings, small cross sections or kinematic limitations.

Closely related to the pion field is the axial vector current of the weak interaction. This is the field that governs the Gamow-Teller beta decay. Its divergence is proportional to the pion field, according to a phenomenological relationship of strong interaction physics. Our present knowledge of the Gamow-Teller transition strength in nuclei is due primarily to nucleon scattering. Beta decay has a narrow energy window that misses the largest states in the spectrum. These states are only found experimentally by the charge exchange nucleon scattering reactions.

There is always a difficulty in using strongly interacting projectiles to probe structure. The various aspects of the collision process must be well understood before quantitative information about target properties can be extracted. First of all, the primary interaction between the projectile and the constituents of the target must be known. Fortunately for nuclear scattering, the empirical knowledge of the interaction deduced from extensive studies of free nucleon-nucleon scattering seems to be adequate for the needs of nuclear structure. The phase shift representation provides the meeting ground between the phenomenology of nucleon-nucleon scattering and the interactions used in more complicated circumstances. The description of the free interaction is the topic of § 2 of the review.

Given the fundamental interaction, the next task is to find the scattering on complex nuclei. All analyses from this point are based on the distorted wave impulse approximation (DWIA). The DWIA approach begins by separating the scattering problem into a reaction part and a target structure part. The reaction aspect is solved approximately so that the target structure information can be extracted directly from experiment. In § 3 we review the basic ingredients of the DWIA.

The target structure part of the reaction is conveniently described in the response function formalism of many-particle quantum mechanics. The charge-changing interaction that is manifest in the projectile-target interaction also influences the target response. In § 4 we discuss the interaction in a nuclear medium. This is considerably

more complicated than the projectile interaction for high-energy particles, because the medium has a strong effect on the interaction. The main theoretical lines to discuss this, and the qualitative results, are given in § 4.

The nuclear response to the charge-changing interaction is reviewed in § 5. The response is particularly concentrated in energy for probes that are spatially uniform, carrying no angular momentum. For the spin-independent response, the excitation is a narrow state known as the isobaric analogue state (IAS). It was first seen as a narrow state high in the continuum by means of the (p, n) reaction (Anderson and Wong 1961). For the response to spin-flip interactions, the strength is concentrated in a peak known as the Gamow-Teller (GT) resonance. This resonance was also discovered using the (p, n) reaction (Doering *et al* 1975).

There are a number of useful theoretical techniques for treating the nuclear response. One very successful method is based on mean field theory. This is a useful approach for nuclei whose wavefunctions are reasonably approximated by a single Slater determinant. For nuclei with more complicated wavefunctions, diagonalisation of a large-dimensioned Hamiltonian matrix is the most reliable method to get details of the response. For either case, some simple properties can be deduced from sum rules. In particular, the total GT strength is bounded by a simple sum rule.

We shall find in § 6 that only 60% of the predicted GT strength is observed. The theoretical implications are also discussed. Subnuclear degrees of freedom, including pions and the delta isobar excitation of the nucleon, may act to quench the strength in the spectroscopic region. Also, configuration mixing may shift the strength from low excitation energies to much higher energies, where it would be difficult to observe with the (p, n) reaction. As we shall see, the present experimental data do not permit a definitive answer about the source of the quenching. Finally, we also discuss other charge exchange measurements that complement the (p, n) cross section measurements and provide further information on the charge-changing nuclear response.

2. Free nucleon–nucleon interaction

The interaction between two nucleons is rather complicated to describe, because in principle there are several independent amplitudes, and each of them is a function of scattering angle and energy. The scattering of nucleons is characterised by a quantity, the t matrix, which we shall call the free nucleon interaction. We shall use this word in the sense of an effective interaction that describes the relative wavefunction at large distances without requiring a detailed model of the behaviour at short distances. This interaction is to be clearly distinguished from the nucleon-nucleon potential, which is only useful when incorporated into a wave equation. Potentials will eventually be needed to determine the effects of the nuclear medium on the interaction, and we will discuss that in § 4. But the t matrix interaction and effective interactions are of central importance to nuclear reaction theory.

Nucleon-nucleon scattering is empirically described by the phase shifts in the partial wave expansion of the scattering amplitude. Intensive studies of nucleon-nucleon scattering have provided us with quite reliable partial wave phase shifts up to 1 GeV (Arndt *et al* 1983). Once all the phase shifts are specified, the interaction between nucleons in free particle states is determined. This interaction can be expressed in two equivalent forms, the scattering amplitude M or the t matrix. These quantities

are related by

$$t = -\frac{4\pi\hbar^2}{[m^2+(p/c)^2]^{1/2}}M \tag{2.1}$$

where p is the momentum in the centre-of-mass frame. The scattering matrix M has the dimension of length, and the t matrix has the dimension of a potential in momentum space, i.e. energy times length cubed. The t matrix is very useful in applying the DWIA to inelastic nucleon-nucleus scattering.

There are five independent amplitudes for each scattering angle and isospin channel (Wolfenstein and Ashkin 1952). A representation of M convenient for nuclear reactions is given by MacGregor *et al* (1960), who also give the formulae to obtain M from the phase shifts. They first define a set of amplitudes R in the partial wave representation, i.e. the orbital angular momentum l of the two particles is coupled to the total spin s to form a total angular momentum j. For the channels that are not mixed, namely the singlet ($s=0$) and the triplet ($s=1$) channels with $j=l$, R is given by

$$R_{jj} = \exp(2i\delta_{jj}) - 1. \tag{2.2}$$

For the channels that mix by the tensor force, namely the triplet channels with $l=j-1$ and $l=j+1$, the R amplitudes are defined in terms of the nuclear 'bar' phase shifts as

$$\begin{aligned} R_{j\pm1,j} &= \cos(2\varepsilon_j)\exp(2i\delta_{j\pm1,j}) - 1 \\ R^j &= i\sin(2\varepsilon_j)\exp(i\delta_{j+1,j} + i\delta_{j-1,j}). \end{aligned} \tag{2.3}$$

Arndt *et al* (1983) have generalised these expressions for R to include the effect of inelasticity, which becomes important at laboratory energies above 300 MeV. The corrections for Coulomb phase shifts in proton-proton scattering have been described by Stapp *et al* (1957). The next step is to define the scattering amplitude M in a representation specifying the components m_s and m_s' of the total spin s along the beam axis. It consists of the singlet amplitude M_{ss} and the triplet amplitudes $M_{m_s'm_s}$. The relations to the R amplitudes in terms of associated Legendre functions are given in table 1, which we quote from table II of MacGregor *et al* (1960) with a restored consistent sign convention.

A more convenient representation of M for inelastic scattering is as a sum over the spin operators of the two particles, the so-called Wolfenstein representation. This separates amplitudes that induce spin excitations in the target from those that are spin independent. We follow the notation of MacGregor *et al* (1960) and write this as

$$M = a + c(\sigma_{1N} + \sigma_{2N}) + m\sigma_{1N}\sigma_{2N} + (g-h)\sigma_{1K}\sigma_{2K} + (g+h)\sigma_{1P}\sigma_{2P}. \tag{2.4}$$

The subscripts 1 and 2 refer to the two nucleons, N is the direction perpendicular to the scattering plane, K is along the momentum transfer and P is along the third coordinate axis ($\boldsymbol{P} = \boldsymbol{K} \times \boldsymbol{N}$), which becomes the beam direction for zero momentum transfer. Spin-independent excitations are induced by the amplitudes a and c, while spin excitations require the amplitudes c, m, g or h. The relation between the M amplitudes in table 1 and the Wolfenstein representation is (MacGregor *et al* 1960)

$$\begin{aligned} a &= \tfrac{1}{4}(2M_{11} + M_{00} + M_{ss}) \\ c &= \frac{i\sqrt{2}}{4}(M_{10} - M_{01}) \\ m &= \tfrac{1}{4}(-2M_{1-1} + M_{00} - M_{ss}) \\ g &= \tfrac{1}{4}(M_{11} + M_{1-1} - M_{ss}) \end{aligned} \tag{2.5}$$

Table 1.

$$M_{ss}(\theta,\phi)=\frac{1}{2ik}\sum P_l(\theta)(2l+1)R_l$$

$$M_{11}(\theta,\phi)=\frac{1}{4ik}\sum P_l(\theta)\{(l+2)R_{l,l+1}+(2l+1)R_{l,l}+(l-1)R_{l,l-1}-[(l+1)(l+2)]^{1/2}R^{l+1}-[(l-1)l]^{1/2}R^{l-1}\}$$

$$M_{00}(\theta,\phi)=\frac{1}{2ik}\sum P_l(\theta)\{(l+1)R_{l,l+1}+lR_{l,l-1}+[(l+1)(l+2)]^{1/2}R^{l+1}+[(l-1)l]^{1/2}R^{l-1}\}$$

$$M_{01}(\theta,\phi)=\frac{\sqrt{2}}{4ik}\exp(i\phi)\sum P_l^1(\theta)\left[-\left(\frac{l+2}{l+1}\right)R_{l,l+1}+\left(\frac{2l+1}{l(l+1)}\right)R_{l,l}+\left(\frac{l-1}{l}\right)R_{l,l-1}+\left(\frac{l+2}{l+1}\right)^{1/2}R^{l+1}-\left(\frac{l-1}{l}\right)^{1/2}R^{l-1}\right]$$

$$M_{10}(\theta,\phi)=\frac{\sqrt{2}}{4ik}\exp(-i\phi)\sum P_l^1(\theta)\left[R_{l,l+1}-R_{l,l-1}+\left(\frac{l+2}{l+1}\right)^{1/2}R^{l+1}-\left(\frac{l-1}{l}\right)^{1/2}R^{l-1}\right]$$

$$M_{1-1}(\theta,\phi)=\frac{1}{4ik}\exp(-2i\phi)\sum P_l^2(\theta)\left[\left(\frac{1}{l+1}\right)R_{l,l+1}-\left(\frac{2l+1}{l(l+1)}\right)R_{l,l}+\left(\frac{1}{l}\right)R_{l,l-1}-[(l+1)(l+2)]^{-1/2}R^{l+1}-[(l-1)l]^{-1/2}R^{l-1}\right]$$

$$M_{-1-1}(\theta,\phi)=M_{11}(\theta,-\phi)\qquad M_{01}(\theta,\phi)=-M_{0-1}(\theta,-\phi)$$

$$M_{-11}(\theta,\phi)=M_{1-1}(\theta,-\phi)\qquad M_{10}(\theta,\phi)=-M_{-10}(\theta,-\phi).$$

$$h=\frac{1}{4\cos\theta}(M_{11}-M_{1-1}-M_{00})=\frac{\sqrt{2}}{4\sin\theta}(M_{10}+M_{01}).$$

The two expressions for h show that the six matrix elements of M given in table 1 are related, so that there are only five independent amplitudes, as in the Wolfenstein representation.

There is yet a third representation of the scattering matrix that has recently received attention. This is based on the Dirac wavefunctions for the nucleons, considered as free particles obeying the Dirac equation. The matrix M is then defined in the combined spin space of the Dirac spinors for both particles. There are five relativistic invariants that can be formed from the Dirac matrices. The scattering matrix therefore has the same number of degrees of freedom as in the representation mentioned above, even though it is expressed in a much larger matrix space, since the Dirac wavefunctions have four components. Specifically, the Dirac representation is (McNeil *et al* 1983)

$$M=F_S+F_V\gamma_1^\mu\gamma_{2\mu}+F_T\sigma_1^{\mu\nu}\sigma_{2\mu\nu}+F_p\gamma_1^5\gamma_2^5+F_A\gamma_1^5\gamma_1^\mu\gamma_2^5\gamma_{2\mu} \tag{2.6}$$

where the different terms transform in the space of each particle as a scalar, vector, tensor, pseudoscalar and axial vector respectively. McNeil *et al* display the matrix to transform from this representation to the Wolfenstein representation. Other invariants can be formed combining Dirac matrices with momentum vectors, as was done in the Wolfenstein representation using Pauli matrices and direction vectors. These can be included with a view to an improved description of the nucleon-nucleus interaction, but the transformation is then no longer unique (Tjon and Wallace 1985a).

2.1. Spin-isospin representation

The different modes of excitation in inelastic nucleon-nucleus scattering are characterised by the spin S and the isospin T of the target excitation. We shall discuss the connection between elastic nucleon-nucleon scattering and inelastic nucleon-nucleus scattering in more detail in the following sections, but it is convenient here to present the elastic nucleon-nucleon scattering in a representation that is associated with the excitation of target modes. From the elastic amplitudes for proton-proton ($M_{\rm pp}$) and proton-neutron ($M_{\rm pn}$) scattering we therefore construct an isoscalar ($T=0$) and an isovector ($T=1$) amplitude:

$$M_{T=0}=(M_{\rm pp}+M_{\rm pn})/2 \qquad M_{T=1}=(M_{\rm pp}-M_{\rm pn})/2. \tag{2.7}$$

These scattering amplitudes are again parametrised as in equation (2.4) in terms of the Pauli spin matrices of the two nucleons. Note that this isospin representation is different from the isospin of the two-nucleon system that is normally used to describe nucleon-nucleon scattering.

We now give the cross sections associated with the different spin-isospin channels. The isospin dependence is suppressed in the notation, since it enters trivially via the constructions in equation (2.7). For $S=0$, i.e. no spin flip of the target nucleons, the only part of M that contributes is $M_{S=0}=a+c\sigma_{1N}$, where the subscript 1 refers to the projectile. Thus we obtain the cross section

$$\left(\frac{{\rm d}\sigma}{{\rm d}\Omega}\right)_{S=0}=|a|^2+|c|^2. \tag{2.8}$$

There are three contributions to $S=1$ excitations, namely a longitudinal, with the spin transfer along the momentum transfer direction K,

$$\left(\frac{{\rm d}\sigma}{{\rm d}\Omega}\right)^{K}_{S=1}=|g-h|^2 \tag{2.9a}$$

and two transverse; one in the scattering plane along the P direction,

$$\left(\frac{{\rm d}\sigma}{{\rm d}\Omega}\right)^{P}_{S=1}=|g+h|^2 \tag{2.9b}$$

and one perpendicular to the scattering plane in the N direction,

$$\left(\frac{{\rm d}\sigma}{{\rm d}\Omega}\right)^{N}_{S=1}=|m|^2+|c|^2. \tag{2.9c}$$

The total $S=1$ cross section is the sum

$$\left(\frac{{\rm d}\sigma}{{\rm d}\Omega}\right)_{S=1}=|g-h|^2+|g+h|^2+|m|^2+|c|^2. \tag{2.10}$$

The so-called spin-flip cross section, measured for example by Nanda *et al* (1983), includes all spin excitations in the scattering plane:

$$\left(\frac{{\rm d}\sigma}{{\rm d}\Omega}\right)_{\rm S\text{-}f}=|g-h|^2+|g+h|^2. \tag{2.11}$$

The nuclear responses associated with spin excitations in the longitudinal direction, equation (2.9*a*), and in the in-plane transverse direction, equation (2.9*b*), have been studied by Carey *et al* (1984).

The equations given above for the spin-dependent cross sections cannot immediately be used for (p, n) exchange reactions. In this case we have to perform both a spatial

exchange and a spin exchange in the pn scattering amplitude. The spatial exchange replaces the scattering angle θ by $\pi - \theta$ in the partial wave expansion. The spin exchange alters the sign of the singlet part of the scattering amplitude, whereas the triplet part is unchanged. If the nucleon-nucleon interaction is charge independent, and in particular independent of the Coulomb interaction, one finds that the elastic (p, n) charge exchange cross sections are identical to four times those given above for the $T = 1$ isovector channel; the only difference is that the longitudinal and the transverse in-plane, i.e. the K and P directions, are interchanged.

2.2. *Empirical properties of the free t matrix*

The t matrix is the most convenient representation of the interaction for application to inelastic scattering, so we shall discuss the physical properties of the empirical nucleon-nucleon interaction in terms of the t matrix. It is related to the scattering amplitude M by the simple numerical factor given in equation (2.1). The spin and isospin decomposition of the t matrix interaction is therefore proportional to the decomposition of the scattering amplitude discussed in the previous section. We shall use the following notation for the t matrix interactions associated with the different spin-isospin excitations of the target: t_0 for isoscalar ($T = S = 0$), t_σ for spin-isoscalar ($T = 0$, $S = 1$), t_τ for isovector ($T = 1$, $S = 0$) and $t_{\sigma\tau}$ for spin-isovector ($T = S = 1$) excitations. An extensive study of the t matrix and its representation by an effective interaction in coordinate space has been made by Love and Franey (1985). We display in figure 1 the t matrix for zero-degree scattering, which has only three degrees of freedom for each isospin (one singlet and two triplet, namely along the beam axis and perpendicular to the beam). This t matrix was obtained from the Arndt phase shifts for $j < 7$ (Arndt *et al* 1983), supplemented with phase shifts from one-pion exchange in higher partial waves ($j > 6$).

The most important feature of the t matrix at low energies is the large attraction in the scalar amplitude and the much smaller repulsion in the other amplitudes. At the lowest energies, the interaction gives a bound state in the coupled $^3S_1 + {}^3D_1$ channel and a quasi-bound state in the $^1S_0$ channel. Then a rough approximation to the t matrix interaction is a short-range attraction that does not depend much on the spin coupling. Such an interaction has the qualitative features noted above for the target excitation amplitudes, namely a strong isoscalar attraction and weak repulsion in the three spin and isospin channels. The repulsive amplitudes at low energy can be viewed as exchange effects of the intrinsically attractive interaction (see below). As the energy increases, the scalar channel attraction decreases and reaches a minimum around 300 MeV. At higher energies the scalar t matrix increases in magnitude due to a growing amplitude from inelastic processes.

The isovector interaction t_τ starts out repulsive and decreases rapidly at higher energies. This behaviour is qualitatively understood as follows. There is no meson that couples strongly to the isovector density, so the interaction will be weak at higher energies. At low energy, however, the exchange interaction from other parts of the interaction contribute to this channel. For example, a pion exchanged with a momentum of the beam momentum produces an amplitude in the isovector channel as well as in other channels. The effect is important at low energies but disappears as the beam momentum increases.

The spin-isovector interaction $t_{\sigma\tau}$ is the most important component of the charge-changing interaction at all but the lowest energies. The spin longitudinal component

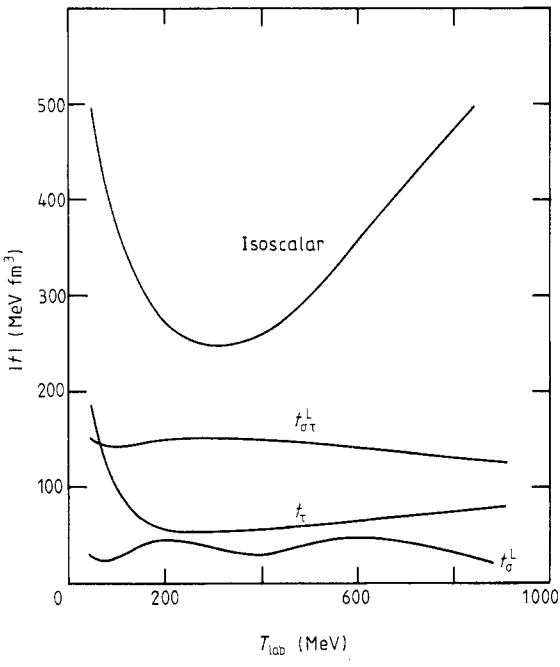

Figure 1. Energy dependence of different components of the t matrix for free nucleon-nucleon scattering at zero momentum transfer. The spin-isospin representation is associated with target excitations.

$t^L_{\sigma\tau}$ (i.e. the spin transfer is along the momentum transfer direction) is fairly constant with a modulus of about 150 MeV fm^3. This may be roughly understood in terms of the direct pion exchange interaction. In the pure one-pion exchange potential model the amplitude as a function of momentum transfer q is

$$V^{\mathrm{OPE}} = -J_\pi \frac{(\boldsymbol{\sigma}_1 \cdot \boldsymbol{q})(\boldsymbol{\sigma}_2 \cdot \boldsymbol{q})}{q^2 + m_\pi^2} \tag{2.12}$$

where m_π is the pion mass and

$$J_\pi = f_\pi^2 \frac{(\hbar c)^3}{(m_\pi c^2)^2} \boldsymbol{\tau}_1 \cdot \boldsymbol{\tau}_2 \simeq 400 \text{ MeV fm}^3 \, \boldsymbol{\tau}_1 \cdot \boldsymbol{\tau}_2 .$$

This vanishes for forward scattering, contrary to the empirical t matrix. However, the amplitude (2.12) is a Born approximation, which is not valid for strong potentials. The potential is strong at small distances, so it is convenient to convert it to coordinate space and solve the Schrödinger equation to find the t matrix. The coordinate space decomposition can be anticipated by writing the q dependence of V^{OPE} as

$$\frac{(\boldsymbol{\sigma}_1 \cdot \boldsymbol{q})(\boldsymbol{\sigma}_2 \cdot \boldsymbol{q})}{q^2 + m_\pi^2} = -\frac{m_\pi^2}{3} \frac{\boldsymbol{\sigma}_1 \cdot \boldsymbol{\sigma}_2}{q^2 + m_\pi^2} + \frac{(\boldsymbol{\sigma}_1 \cdot \boldsymbol{q})(\boldsymbol{\sigma}_2 \cdot \boldsymbol{q}) - \frac{1}{3} q^2 \boldsymbol{\sigma}_1 \cdot \boldsymbol{\sigma}_2}{q^2 + m_\pi^2} + \tfrac{1}{3} \boldsymbol{\sigma}_1 \cdot \boldsymbol{\sigma}_2 . \tag{2.13}$$

The first term is the ordinary Yukawa interaction and the second term is the tensor interaction. The third term is a contact interaction which in coordinate space becomes a delta function at the origin. When the Schrödinger equation is solved, the delta function at the origin has no effect on the wavefunction. Indeed, other short-range repulsive interactions will keep the particles apart, so this term in the pionic interaction

will not be felt. If we assume that the finite-range parts of the interaction (2.13) are well enough behaved to apply the Born approximation, the end result is that the contact term is ineffective. The remaining part of the direct interaction is

$$V_\pi^{\mathrm{D}}(\boldsymbol{q}) = -J_\pi \left(\frac{(\boldsymbol{\sigma}_1 \cdot \boldsymbol{q})(\boldsymbol{\sigma}_2 \cdot \boldsymbol{q})}{q^2 + m_\pi^2} - \tfrac{1}{3} \boldsymbol{\sigma}_1 \cdot \boldsymbol{\sigma}_2 \right). \tag{2.14}$$

This has a value of 133 MeV fm^3 at $q = 0$, which is the same order of magnitude as the empirical t matrix at that momentum transfer. Also, it is relatively independent of energy, suggesting that the one-pion exchange interaction is responsible for most of the physics of the excitation process in the longitudinal spin-isovector channel.

It is interesting to look at the ratio of the $t_{\sigma\tau}^{\mathrm{L}}$ to the t_τ interaction strength, as this will show the selectivity of the scattering for spin or spin-independent excitations. This is shown in figure 2. As first pointed out by Love and Franey (1981, 1983), this ratio peaks at an energy of about 300 MeV, making this a good beam energy to study spin excitations in (p, n) reactions. Figure 2 also shows the empirical ratio extracted from comparison of excitation cross sections on nuclear targets. This will be discussed in § 3.

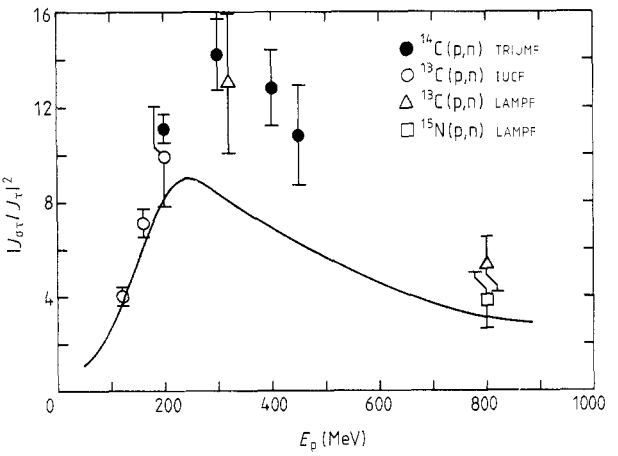

Figure 2. Energy dependence of the ratio of the isovector spin-longitudinal and the isovector t matrix interactions at zero momentum transfer. The full curve is based on the Arndt *et al* (1983) phase shifts supplemented by one-pion exchange for the high partial waves. The data points, obtained from Alford *et al* (1986), are determined by comparing the forward-angle exchange cross sections for nuclear states with known properties. (Used with the permission of the authors prior to publication.)

Because the nuclear interaction has a tensor force component, the $S = 1$ amplitudes depend on orientation, cf equations (2.9*a–c*). For forward scattering, the orientations along the beam and perpendicular to the beam direction are independent, whereas the longitudinal direction and the transverse direction perpendicular to the scattering plane become indistinguishable in this limit. The t matrices with the spin oriented along the beam direction are shown in figure 3. The magnitudes are comparable with the interactions in other spin directions. The fact that there is some difference shows that the tensor interaction can play some role even at zero degrees.

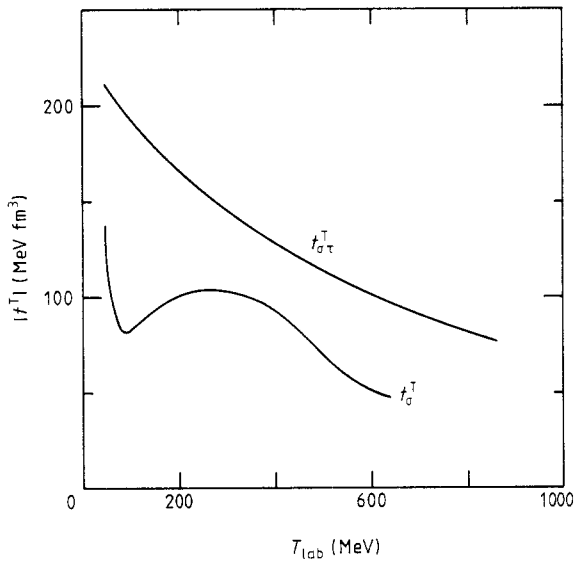

Figure 3. Energy dependence of the spin-transverse isoscalar and isovector t matrix at zero momentum transfer. The transverse spin operators are parallel to the beam direction.

2.3. The t matrix at finite q

The cross section at low energy is close to isotropic apart from Coulomb effects, consistent with the rough characterisation of the t matrix interaction as a short-range attraction. The angular distribution for identical particle scattering remains flat up to fairly high energies, but this is deceptive because the various spin amplitudes contribute differently at different scattering angles. In charge exchange scattering, there is a peak in the differential cross section at zero degrees (i.e. at 180° in elastic np scattering) that persist to multi-GeV energies. An example of this peaking for small momentum transfers in charge exchange is shown in figure 4, which displays the differential cross

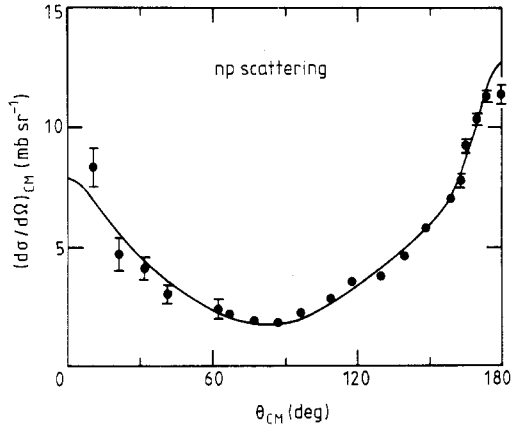

Figure 4. Elastic np scattering at 200 MeV. The data are from Kazarinov and Simonov (1963), and the calculated curve is obtained from the Arndt *et al* (1983) phase shifts. Note the sharp peak at 180° scattering.

section for np scattering at 200 MeV in the laboratory. The variation of the cross section near $q = 0$ (i.e. near 180° in figure 4) is associated with one-pion exchange but, as we saw in the previous section, the behaviour is not as simple as the Born approximation expression. The naive pion exchange process is zero at $q = 0$, but the rescattering and short-range correlations make the amplitude finite and give a q dependence like (2.14). The amplitude is sharply peaked at $q = 0$ for the spin component parallel to $\boldsymbol{q}$. This is the longitudinal spin-flip amplitude; in the Wolfenstein representation, equation (2.4), it is given by the combination of amplitudes $g - h$. Figure 5(a) shows the longitudinal isovector t matrix $t^{\mathrm{L}}_{\sigma\tau}$ as a function of q. The t matrix is repulsive for small q, and changes sign at larger q.

There are three other spin amplitudes transverse to $\boldsymbol{q}$ when q is finite. In order to discuss the physics underlying the transverse spin-isovector t matrix, it is convenient to regroup the transverse part of (2.4) and express it as

$$M^{\mathrm{T}}_{\sigma\tau} = c\sigma_{2N} + \tfrac{1}{2}(m+g+h)(\sigma_{1N}\sigma_{2N} + \sigma_{1P}\sigma_{2P}) + \tfrac{1}{2}(m-g-h)(\sigma_{1N}\sigma_{2N} - \sigma_{1P}\sigma_{2P}). \quad (2.15)$$

The three corresponding t matrix interactions are shown in figure 5(b). The first term

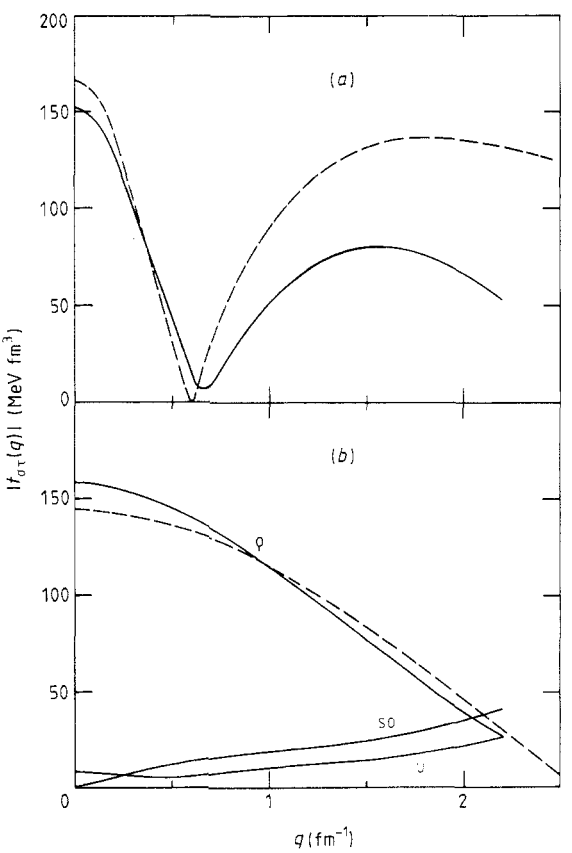

Figure 5. Isovector spin-longitudinal (a) and spin-transverse (b) t matrix at 200 MeV as functions of the momentum transfer; the transverse components are defined in equation (2.15). The full curves were obtained from the Arndt phase shifts and the broken curves represent the result of the $\pi + \rho$ model as explained in § 2.4.

is associated with the spin-orbit interaction and is denoted by so in the figure. The second term (denoted by ρ) can arise from the ρ meson exchange, using the magnetic-type coupling $(\boldsymbol{\sigma}_1 \times \boldsymbol{q}) \cdot (\boldsymbol{\sigma}_2 \times \boldsymbol{q})$ to the ρ meson. The last term (denoted by U) can only arise from non-local interactions and exchange effects. The ρ-like amplitude is dominant at all but the highest momentum transfers.

2.4. $\pi + \rho$ model

The one-pion exchange model is too crude to use as an approximation to the complete spin-isovector t matrix. The longitudinal t matrix falls off too quickly and is too attractive at large q, making it a poor fit to the t matrix interaction shown in figure 5(a). A more accurate representation can be constructed by adding ρ meson exchange to the pion exchange. This has been done by the Jülich-Stony Brook groups with the '$\pi + \rho$ model' (Speth 1980), which we now describe. The basic idea is the same as previously mentioned, namely to cut away the contact interaction, which is not effective in the presence of other short-range repulsive interactions. The ρ meson exchange force is taken to be

$$V_\rho(\boldsymbol{q}) = -J_\rho \frac{(\boldsymbol{\sigma}_1 \times \boldsymbol{q}) \cdot (\boldsymbol{\sigma}_2 \times \boldsymbol{q})}{q^2 + m_\rho^2} \tag{2.16}$$

where m_ρ is the ρ meson mass and

$$J_\rho = f_\rho^2 \frac{(\hbar c)^3}{(m_\rho c^2)^2} \boldsymbol{\tau}_1 \cdot \boldsymbol{\tau}_2 \simeq 790 \text{ MeV fm}^3 \, \boldsymbol{\tau}_1 \cdot \boldsymbol{\tau}_2.$$

We shall repeatedly use the relation

$$\boldsymbol{q}^2 \boldsymbol{\sigma}_1 \cdot \boldsymbol{\sigma}_2 = (\boldsymbol{\sigma}_1 \cdot \boldsymbol{q})(\boldsymbol{\sigma}_2 \cdot \boldsymbol{q}) + (\boldsymbol{\sigma}_1 \times \boldsymbol{q}) \cdot (\boldsymbol{\sigma}_2 \times \boldsymbol{q}). \tag{2.17}$$

Similar to the π exchange, the ρ exchange interaction can then be decomposed into a tensor force, a Yukawa-type interaction and a contact interaction:

$$V_\rho = J_\rho \left(\frac{(\boldsymbol{\sigma}_1 \cdot \boldsymbol{q})(\boldsymbol{\sigma}_2 \cdot \boldsymbol{q}) - \frac{1}{3} q^2 \boldsymbol{\sigma}_1 \cdot \boldsymbol{\sigma}_2}{q^2 + m_\rho^2} + \frac{2}{3} \frac{m_\rho^2 \boldsymbol{\sigma}_1 \cdot \boldsymbol{\sigma}_2}{q^2 + m_\rho^2} - \tfrac{2}{3} \boldsymbol{\sigma}_1 \cdot \boldsymbol{\sigma}_2 \right). \tag{2.18}$$

Notice that the tensor forces tend to cancel between the π and the ρ contributions, whereas the Yukawa interactions have the same sign. The ρ exchange interaction is next modified to account for correlation effects. Speth *et al* drop the contact term and reduce the Yukawa term by a factor of $\gamma = 0.4$. Leaving the tensor part unchanged, they find the following expression for the direct ρ exchange interaction:

$$V_\rho^{\mathrm{D}} = -J_\rho \left[\frac{(\boldsymbol{\sigma}_1 \times \boldsymbol{q}) \cdot (\boldsymbol{\sigma}_2 \times \boldsymbol{q})}{q^2 + m_\rho^2} - \frac{2}{3} \left((\gamma - 1) \frac{m_\rho^2}{q^2 + m_\rho^2} + 1 \right) \boldsymbol{\sigma}_1 \cdot \boldsymbol{\sigma}_2 \right]. \tag{2.19}$$

One can now extract the direct longitudinal $(\boldsymbol{\sigma}_1 \cdot \boldsymbol{q})(\boldsymbol{\sigma}_2 \cdot \boldsymbol{q})$ and transverse $(\boldsymbol{\sigma}_1 \times \boldsymbol{q}) \cdot (\boldsymbol{\sigma}_2 \times \boldsymbol{q})$ components from the modified direct π and ρ exchange interactions (equations (2.14) and (2.19)). We do not show the explicit expressions here but refer the reader to Love *et al* (1984). These authors also include the nucleon exchange terms, as minus a quarter of the direct interactions evaluated at the beam momentum. They furthermore include a contact term V_c in order to make this model a more quantitative parametrisation of the physical t matrix.

In figures 5(*a*) and (*b*) we display the interactions obtained from the '$\pi+\rho$' model (broken curves). A momentum-independent contact interaction of $V_c = 162$ MeV fm^3 has been added to fit the free t matrix at small momentum transfers. The model reproduces the transverse channel $(\boldsymbol{\sigma}_1 \times \boldsymbol{q}) \cdot (\boldsymbol{\sigma}_2 \times \boldsymbol{q})$ quite well, but it is not so successful in the spin-longitudinal channel at large momentum transfers. This is perhaps to be expected, since the pion exchange interaction is long range, and corrections to it that go mainly into the longitudinal channel could have some residual q dependence.

3. Distorted wave impulse approximation

Given the interaction between the projectile and the target nucleons, the excitation cross sections are calculated in the impulse approximation (Kerman *et al* 1959). This assumes that the interaction only acts in first order to make the transition between target states. The interaction also has diagonal matrix elements in the target state. This part of the interaction is included to all orders in constructing the scattering wavefunctions, making them distorted waves.

The basic equation for the inelastic cross section (in the centre-of-mass frame) is given by the distorted wave impulse approximation (DWIA; see Haybron and MacManus 1964, 1965)

$$\frac{\mathrm{d}^2\sigma}{\mathrm{d}\Omega\,\mathrm{d}E} = \left(\frac{\mu}{2\pi\hbar^2}\right)^2 \sum_n \frac{k_n}{k_0} |\langle \psi_n \phi_{p'} | V_{\mathrm{pt}} | \psi_0 \phi_{\mathrm{p}} \rangle|^2 \delta(E - \varepsilon_{n0}). \tag{3.1}$$

Here ϕ_{p} and $\phi_{\mathrm{p}'}$ are the distorted waves of the projectile in the initial and final states, respectively, and ψ_0 and ψ_n are the associated many-particle wavefunctions of the two target states. The off-diagonal part of the interaction that is responsible for the excitation is denoted by V_{pt} and μ is the reduced mass. If the interaction were given by a two-body potential, the expression would clearly be the distorted wave Born approximation. However, the nucleon–nucleon interaction is too strong to use a Born approximation, so V_{pt} is supposed to represent an effective interaction. The impulse approximation, as originally formulated by Kerman *et al* (1959), uses the free nucleon–nucleon t matrix for this effective interaction. The empirical knowledge of the t matrix is limited to free particle states with the appropriate on-energy-shell relations between momentum and energy, but the matrix element above requires much more information about the t matrix. The most justified method for producing an effective interaction requires first determining a true potential that is consistent with the free nucleon–nucleon scattering. The t matrix constructed from the potential would have diagonal as well as off-diagonal components. In the integral equation that determines the t matrix from the potential, some of the effects of the nuclear medium could be incorporated, as discussed in § 4.

It is common to disregard the full non-locality of the t matrix and to use a local interaction in coordinate space for (3.1). The direct plus exchange matrix elements of this interaction, evaluated for plane wave states, should reproduce the known t matrix elements. A potential of this kind, based on the free scattering t matrix, has been constructed by Love and Franey (1985). The interaction is represented in coordinate space by a sum of Yukawa functions. An earlier study by Bertsch *et al* (1977) determined an effective interaction for low-energy projectiles, with medium effects incorporated by fitting matrix elements of the Brueckner theory (see § 4). The latter were given in a harmonic oscillator basis and the effective interaction was also a sum of Yukawa functions.

The Yukawa functions are convenient for numerical evaluations of matrix elements, since they can be represented in a separable form in terms of modified Bessel functions:

$$Y(|\boldsymbol{r}_1-\boldsymbol{r}_2|)=\frac{1}{(r_1r_2)^{1/2}}\sum_{L=0}(2L+1)I_{L+1/2}(r_<)K_{L+1/2}(r_>)P_L(\cos\theta_{12}). \quad (3.2)$$

A computer code DWBA70 based on Yukawa potentials has been constructed by Schaeffer and Raynal (Raynal 1967), and it is the commonly used code for the most detailed calculations. This code makes it possible to calculate the exchange interaction exactly, given the structure of the target wavefunction. For most applications, the exchange interaction does not have to be calculated exactly, since a local approximation in terms of a delta function interaction is fairly accurate (Petrovich *et al* 1969).

The diagonal part of the nucleon-nucleus interaction is usually treated phenomenologically in an optical model, and the distorted waves of the projectile are calculated by solving the Schrödinger equation. The optical potential includes an imaginary part that serves to attenuate the projectile wavefunction in the interior of the target. In principle, the optical potential can be calculated from Brueckner theory, to be described in § 4 (Jeukenne *et al* 1976, Brieva and Rook 1978). However, these calculations are not as reliable as an empirical determination from elastic scattering data. Even at the level of empirical determination, there is considerable ambiguity in the optical potential (Kobas *et al* 1982, Meyer and Schwandt 1981, Meyer *et al* 1981). Elastic scattering at intermediate energies can be fitted with a potential having a monotonic real part and a relatively weak absorptive part (Nadasen *et al* 1981), or a potential with a stronger absorption but a real part having a more complicated shape. Satchler (1983) showed that predicted inelastic cross sections can differ by as much as a factor of two using the different kinds of potentials.

At high energies one expects the medium corrections to the t matrix to be small and the optical potential could be determined from the free t matrix. However, the non-relativistic t matrix fails to reproduce some properties of the potential at intermediate energies. In particular, there is a difference in the shape between the central and spin-orbit potential that is responsible for diffractive structures in spin observables (Clark *et al* 1983). This feature of the optical potential is much better described by relativistic models and the potential can be related to the t matrix expressed in a Dirac representation (Tjon and Wallace 1985b).

3.1. Spectroscopic applications of the (p, n) reaction

The (p, n) reaction has been a very useful spectroscopic tool because the reaction mechanism is well described by the DWIA at all but the lowest beam energies. The angular distribution has considerable diffraction structure, which allows the orbital angular momentum of the states to be determined. Also, the relative cross sections to different states are closely related to their intrinsic response to charge-changing fields.

The (p, n) reaction first gained prominence at low beam energies where the main spectroscopic information was related to the isobaric analogue state (IAS). In more recent applications with intermediate-energy protons, the spin transitions become dominant and the distorted waves simplify. In particular, the spin transitions with $L=0$ (i.e. no angular momentum transfer) are closely related in the (p, n) reaction and in beta decay, where they are known as Gamow-Teller transitions. The DWIA allows a semi-quantitative extraction of the Gamow-Teller matrix elements from the

forward-angle cross sections (Goodman *et al* 1980). We now show how this reduction is made.

First, the interaction in equation (3.1) is treated as a momentum-dependent contact interaction. Then the matrix element to be evaluated can be expressed by

$$\begin{aligned}\langle\psi_n\phi_{p'}|V_{pt}|\psi_0\phi_p\rangle &= t_{\sigma\tau}(q)\langle\psi_n\phi_{p'}|\delta^{(3)}(\boldsymbol{r}_p-\boldsymbol{r}_t)(\boldsymbol{\sigma}_p\cdot\boldsymbol{\sigma}_t)(\boldsymbol{\tau}_p\cdot\boldsymbol{\tau}_t)|\psi_0\phi_p\rangle \\ &= t_{\sigma\tau}(q)\int d^3\boldsymbol{r}\rho^p_{\sigma\tau}(\boldsymbol{r})\rho^t_{\sigma\tau}(\boldsymbol{r})\end{aligned} \tag{3.3}$$

where $\rho_{\sigma\tau}(\boldsymbol{r})$ are transition densities for the $\sigma\tau$ operators in the target and projectile, respectively, and $t_{\sigma\tau}(q)$ is the associated t matrix at the momentum transfer q.

The projectile transition density is essentially the product of incoming and outgoing projectile wavefunctions:

$$\rho^p_{\sigma\tau}(\boldsymbol{r}) \simeq \phi^*_{p'}(\boldsymbol{r})\phi_p(\boldsymbol{r})\langle p'|\sigma\tau|p\rangle. \tag{3.4}$$

For forward scattering and not too large energy transfers, this density has a nearly constant phase over the nuclear volume, although its magnitude of course varies due to the absorption in the optical potential. The transition density for the target determines the Gamow-Teller (GT) matrix element for the transition:

$$M_{GT}(0\to n) = \int d^3\boldsymbol{r}\rho^t_{\sigma\tau}(\boldsymbol{r}) = \langle\psi_n|\sigma\tau|\psi_0\rangle. \tag{3.5}$$

Furthermore, it is convenient to define a factor that contains the effect of the absorption:

$$N_D = \left|\int d^3\boldsymbol{r}\,\rho^p_{\sigma\tau}(\boldsymbol{r})\rho^t_{\sigma\tau}(\boldsymbol{r})/M_{GT}(0\to n)\right|^2. \tag{3.6}$$

The main dependence on structure has been extracted via the GT matrix element M_{GT}. To the extent that all transitions have the same radial shape, the absorption factor N_D will be independent of the transition. If there were no distortion of the scattering wavefunction, the absorption factor would be unity for forward scattering. With these definitions we finally arrive at the following expression for the zero-degree cross section for individual GT transitions:

$$\left(\frac{d\sigma}{d\Omega}\right)_n = \left(\frac{\mu}{2\pi\hbar^2}\right)^2 |t_{\sigma\tau}(0)|^2 N_D \frac{k_n}{k_0}|M_{GT}(0\to n)|^2. \tag{3.7}$$

The cross section for the isobaric analogue state (IAS)—the so-called Fermi transition generated by the isovector interaction t_τ—is given by a similar expression. Knowing the normalisation factor N_D makes it possible to extract the GT and the Fermi transition matrix elements directly from measured zero-degree (p, n) cross sections. This method has been applied by Goodman *et al* (1980) to show the close relationship between transitions in (p, n) reactions and in beta decay over the entire range of nuclei where strong transitions can be compared. However, if the beta decay transition is weak, the method becomes unreliable. The (p, n) cross section is not reduced to the same extent as the beta decay rate for very weak transitions (Watson *et al* 1985).

Typical (p, n) spectra taken at different beam energies are shown in figure 6. Both the GT and the IAS are seen in the spectra. They are both $\Delta l = 0$ transitions. The spin excitation makes the GT a 1^+ state, whereas the IAS is a 0^+ state. The IAS is the strongest state at the lowest energy and the GT state is dominant at 200 MeV. This behaviour is consistent with the strong energy dependence of the t matrix interactions (Love and Franey 1981) as illustrated in figure 2.

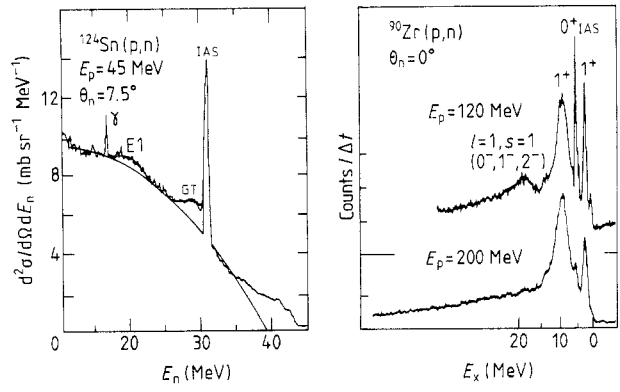

Figure 6. Neutron spectra in (p, n) reactions at different beam energies; at 45 MeV on ^{124}Sn (from Sterrenburg *et al* 1980), and at 120 and 200 MeV on ^{90}Zr (from Gaarde 1983). (Used with the permission of the authors and North-Holland Publishing Company.)

3.2. Eikonal approximation

The DWIA calculations are rather time-consuming, so it is useful to have simpler expressions that display the main features of the cross section. Further simplifications can be achieved at higher beam energies, where the eikonal approximation applies, and where the influence of the real part of the optical potential can be ignored. The transition density associated with the projectile and the detected nucleon can then be estimated by

$$\rho^{\mathrm{p}}(\boldsymbol{r}) = \exp(-\mathrm{i}\boldsymbol{q}\cdot\boldsymbol{r}) \exp\left(-\frac{1}{\hbar v_0}\int_{-\infty}^{\infty} \mathrm{d}z\, W(r)\right) \tag{3.8}$$

where $W(r)$ is the imaginary part of the optical potential and v_0 is the beam velocity. The z integration is along an axis parallel to the beam direction, and we have neglected the dependence on excitation energy (Q value) for simplicity. For low excitations and forward scattering, the momentum transfer $\boldsymbol{q}$ is perpendicular to the beam direction. This transition density is a function of the transverse coordinate vector $\boldsymbol{b}$, which in the classical limit plays the role of an impact parameter. If the absorption is strong, the attenuation factor from the optical potential implies that the major contributions to the matrix element (3.3) are localised in a narrow ring around the target nucleus.

In this section we consider transitions that are more general than the GT. The transitions can be generated by the $\sigma\tau$ or the τ operator, and we include a dependence on the angular momentum transfer in the transition density for target excitations:

$$\rho^{\mathrm{t}}_{n\lambda\mu}(\boldsymbol{r}) = \langle n\lambda\mu|\rho^{\mathrm{t}}|0\rangle = \delta\rho_{n\lambda}(r)\, Y^*_{\lambda\mu}(\theta, \phi)/(2\lambda+1)^{1/2}. \tag{3.9}$$

Our treatment of the angle dependence of the inelastic cross section is similar to that of Blair (1959). The ϕ angle is the azimuthal angle around the beam axis. The integration over ϕ in (3.3) involves

$$\int_0^{2\pi} \mathrm{d}\phi\, \exp(-\mathrm{i}\mu\phi) \exp(-\mathrm{i}qb\cos\phi) = 2\pi J_\mu(qb). \tag{3.10}$$

If the main contribution in (3.3) arises from $b \simeq R$ and $\theta \simeq \pi/2$, we can extract this factor and obtain the approximation

$$\langle \psi_n \phi_{\mathrm{p}'} | V_{\mathrm{pt}} | \psi_0 \phi_{\mathrm{p}} \rangle \simeq t(q)\, Y^*_{\lambda\mu}(\pi/2, 0) J_\mu(qR) M_{n\lambda} N_{\mathrm{D}} \tag{3.11}$$

where $M_{n\lambda}$ is defined similar to (3.5),

$$M_{n\lambda} = \int \mathrm{d}^3\boldsymbol{r}\, \delta\rho_{n\lambda}(r)/(2\lambda+1)^{1/2} \tag{3.12}$$

and N_D is the normalisation factor, determined by the attenuation of the projectile wavefunction inside the target nucleus,

$$N_D = \left| \int \mathrm{d}^3\boldsymbol{r}\, \delta\rho_{n\lambda}(r) \exp\left(-\frac{1}{\hbar v_0} \int_{-\infty}^{\infty} \mathrm{d}z W(r) \right) M_{n\lambda}^{-1} \right|^2 . \tag{3.13}$$

These approximations leave us with the following simple expression for the differential cross section:

$$\frac{\mathrm{d}^2\sigma}{\mathrm{d}\Omega\, \mathrm{d}E} = \left(\frac{\mu}{2\pi\hbar^2} \right)^2 \sum_{n,\mu} \frac{k_n}{k_0} |t(q)\, Y_{\lambda\mu}(\pi/2, 0) J_\mu(qR)|^2 N_D |M_{n\lambda}|^2 \delta(E - \varepsilon_{n0}). \tag{3.14}$$

The angle dependence of the cross section is determined by the product of the t matrix and the Bessel function. Thus for a given angular momentum transfer λ, the cross section has a maximum at an angle that is mainly determined by the position of the maximum of the Bessel function. The target dependence enters, of course, via the structure-dependent terms $M_{n\lambda}$ and the position of the excitation energy. These features will be illustrated in the next section. The absorption factor N_D contains the target dependence due to the attenuation of the beam inside the target nucleus. It has a weaker dependence on structure via the transition density and the Q value of the transition. The Q value dependence was suppressed in the approximation (3.8). We now discuss some general features related to the strength of the optical potential.

The weak absorption that is often used to fit elastic scattering, and is associated with a Wood-Saxon parametrisation of the optical potential, implies that the (p, n) reaction probes the transition density over the entire nucleus. For a constant transition density, the absorption factor for central collisions can be estimated by

$$N_D(b=0) = \exp\left(-\frac{4RW(0)}{\hbar v_0} \right) \tag{3.15}$$

where R is the nuclear radius. Neither this estimate nor detailed DWIA calculations with a weak absorption yield the correct absolute magnitude of observed (p, n) cross sections. This point has been investigated for GT transitions that are known from beta decay (Goodman *et al* 1980). The analysis of GT strength in (p, n) reactions has therefore been based on interpolations of the absorption factor between nuclei for which a calibration to known beta transitions can be performed.

The stronger absorption that is associated with a double Wood-Saxon parametrisation of the real part of the optical potential (Meyer *et al* 1981, 1983), implies that the transition density is probed mainly near the surface of the target nucleus and it yields a different value for N_D.

The dependence of the absorption factor on Q value can be expressed as a function of the adiabaticity parameter ξ. This quantity is a product of the excitation energy ΔE and a typical length over which the reaction takes place, divided by the beam velocity. In the weak absorption limit, where the entire nucleus is probed, the adiabaticity parameter is $\xi = 2R\Delta E/\hbar v_0$. For strong absorption the reaction takes place near the surface and the typical length is not $2R$ but $2(2Rd)^{1/2}$, where d is a surface thickness determined by the strength of the absorption. The adiabatic cut-off is therefore sensitive

to the strength of the optical potential. This fact is important for an experimental determination of the total GT strength. Although a substantial strength may be located at higher excitations above the GT resonance, as discussed in § 5, it may not be seen in the (p, n) reactions due to the adiabatic cut-off. It is therefore important to have a realistic optical potential in order to extract the total strength from the measured (p, n) cross sections. It is also desirable to perform the measurements at the highest possible beam energy, since the adiabaticity parameter becomes smaller in this limit.

3.3. Angular distributions

The angular dependences of specific parts of the spectrum observed in (p, n) reactions on ^{90}Zr are shown in figure 7. The angular distributions for the IAS and the GT transitions shown to the left have a maximum at zero degrees, characteristic for $\lambda = 0$ transitions. The distributions to the right have their maximum at a finite scattering angle; they have been assigned to specific shell model transitions as indicated on the figure. The peak positions in angle space are consistent with the formula (3.14) obtained in the eikonal approximation. The maximum of the Bessel function is at $qR = 1.8$ for $\mu = \lambda = 1$ and $qR = 3.1$ for $\mu = \lambda = 2$, corresponding to scattering angles of 6.2 and 10.6° respectively. The t matrix interaction has, of course, also a q dependence, which can shift the peak position to more forward angles, but the simple estimates based on the Bessel functions already show a rough agreement with the data.

An overview of the (p, n) cross section for reactions on ^{90}Zr at 200 MeV is shown in figure 8 as a function of the excitation energy at different scattering angles. The GT

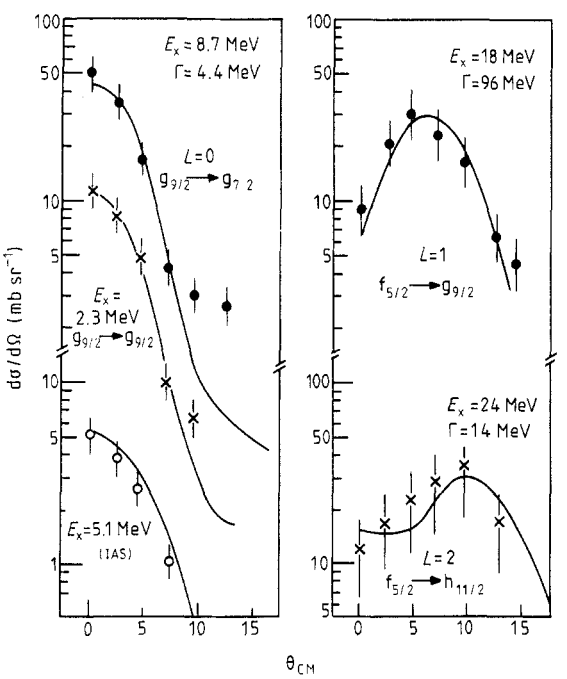

Figure 7. Angular distributions of specific peaks in (p, n) reactions on ^{90}Zr at 200 MeV (from Gaarde *et al* 1981). The curves (with arbitrary normalisation) have been obtained from DWIA calculations for typical single-particle transitions. (Used with the permission of the authors and North-Holland Publishing Company.)

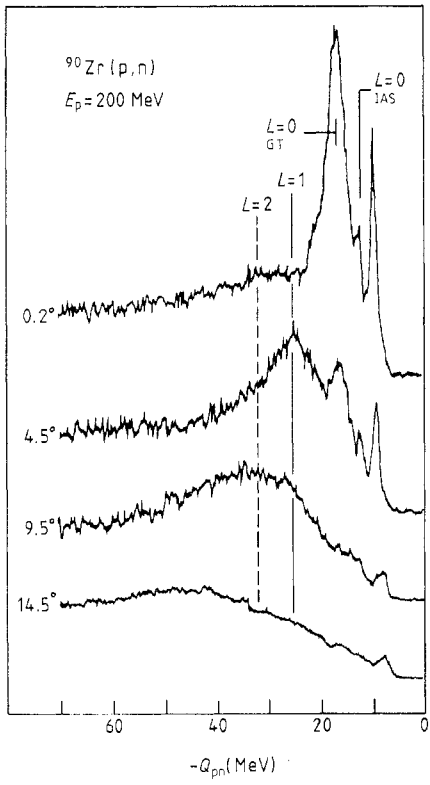

Figure 8. Neutron spectra from (p, n) reactions on ^{90}Zr at 200 MeV; the different scattering angles are indicated (from Gaarde *et al* 1981). (Used with the permission of the authors and North-Holland Publishing Company.)

state is strongly excited at forward angles, whereas the IAS is much weaker at this beam energy. At larger scattering angles the $\lambda = 1$ and $\lambda = 2$ transitions start to dominate the spectra, and at the largest scattering angles the spectrum becomes a broad quasi-elastic peak with no obvious or clear signature of structural transitions.

Osterfeld *et al* (1985) have reproduced all the spectra shown in figure 8 by DWIA calculations. They use the weakly absorbing optical potential of Nadasen *et al* (1981) and the Love and Franey (1981) interaction for the charge exchange. They normalise the cross section by comparing with the known beta decay of ^{42}Ca, finding that the theoretical cross section must be increased by a factor of 1.16. With this model they obtain a good agreement with the data for scattering angles from 0° to 20°. This result suggests that the (p, n) reactions on heavy nuclei are dominated by single-step transitions. This conclusion may be too strong; a certain amount of single scattering will unavoidably introduce contributions from multi-step processes. We shall return to this question in § 6, where we discuss the background of the total GT strength.

4. The interaction in a nuclear medium

The effective interaction of an incoming nucleon and a nucleon bound in a target nucleus is different from the free t matrix interaction. A detailed study of medium

corrections requires as input a potential for the interaction between free nucleons. There are several phenomenological potentials available. The most detailed and commonly used are known as the Paris potential (Lacombe *et al* 1980) and the Bonn potential (Holinde *et al* 1972). These potentials have been constructed to be as consistent with meson exchange theory as possible. The long-range parts are completely local and based on pion exchange. At intermediate range, the Paris potential uses two-meson exchange theory, while the Bonn potentials use heavier mesons. The two-meson exchange in the Paris potential introduces some non-locality that is not present in the Bonn potentials. At short distances, the potentials are completely phenomenological and adjusted to fit the Arndt phase shifts (Arndt *et al* 1983), and thereby the elastic scattering t matrix. Above pion production threshold, no potential model can reproduce the phase shifts for elastic scattering because of the inelasticity.

4.1. Brueckner theory

Once a potential is assumed, the next step is to determine a t matrix that incorporates medium corrections. The Brueckner theory provides the proper treatment of these effects and replaces the free t matrix by the G matrix. For a complete review of the Brueckner theory, the reader is referred to Day (1967) and Bethe (1971). Here we will only describe the theory in broad terms. There are two important kinds of medium corrections that are included in the theory. One is the Pauli principle, which restricts intermediate two-particle states to be above the Fermi level. From the study of the free t matrix we know that it is important to treat the short-range part of the nucleon-nucleon potential to all orders. One can therefore expect that the Pauli blocking in a nuclear medium modifies the effect of the short-range interaction dramatically. A second medium correction in the Brueckner theory is a possible modification of the energy spectrum of two-particle states due to the other particles in the medium.

The fundamental equation determining the G matrix is the Bethe-Goldstone equation. It may be written formally in terms of the free nucleon-nucleon potential V as

$$\langle \mathrm{p}_1'\mathrm{p}_2'|G|\mathrm{p}_1\mathrm{p}_2\rangle = \langle \mathrm{p}_1'\mathrm{p}_2'|V|\mathrm{p}_1\mathrm{p}_2\rangle + \sum_{k_1k_2>k_F} \frac{\langle \mathrm{p}_1'\mathrm{p}_2'|V|k_1k_2\rangle\langle k_1k_2|G|\mathrm{p}_1\mathrm{p}_2\rangle}{E-\varepsilon(k_1,k_2)}. \quad (4.1)$$

Here E is the total available two-particle energy. The initial and final two-particle states are denoted by $|\mathrm{p}_1\mathrm{p}_2\rangle$ and $|\mathrm{p}_1'\mathrm{p}_2'\rangle$. The sum is over intermediate states $|k_1k_2\rangle$ with energy $\varepsilon(k_1, k_2)$. The G matrix equation differs from the Lippmann-Schwinger equation for the t matrix in two respects, as already mentioned: the sum over intermediate states $|k_1k_2\rangle$ is restricted by the Pauli principle to unoccupied states, and the energy of these states differs from the free energy

$$\varepsilon(k_1, k_2) = \frac{\hbar^2}{2m}(k_1^2+k_2^2) \quad (4.2)$$

by the medium corrections to the single-particle energies. In infinite nuclear matter the total momentum $\boldsymbol{k}_1+\boldsymbol{k}_2$ of two interacting particles is conserved; it appears in equation (4.1) merely as a parameter. It is therefore convenient to express this equation in terms of variables for the relative and the centre-of-mass motion respectively:

$$\boldsymbol{k} = (\boldsymbol{k}_1-\boldsymbol{k}_2)/2 \qquad \boldsymbol{K} = (\boldsymbol{k}_1+\boldsymbol{k}_2)/2. \quad (4.3)$$

It is customary to treat both the restriction from the Pauli principle and the single-particle energy spectrum in approximations which allow the G matrix equation to be separated into partial waves for the relative coordinate. The Pauli operator is treated in an angle-averaging approximation

$$\sum_{k_1 k_2 > k_F} |k_1 k_2\rangle\langle k_1 k_2| \sim \sum_{k,K} |Kk\rangle Q_K(k)\langle Kk| \tag{4.4}$$

where $Q_K(k)$ is a scalar function of k. For infinite nuclear matter one finds

$$Q_K(k) = \begin{cases} 0 & \text{if } k^2 + K^2 < k_F^2 \\ 1 & \text{if } |K-k| > k_F \\ (k^2 + K^2 - k_F^2)/2kK & \text{otherwise.} \end{cases} \tag{4.5}$$

The separation between the centre-of-mass and relative motion requires that the single-particle energies are of the form

$$\varepsilon(k) = \frac{\hbar^2}{2m_p} k^2 + U_p \tag{4.6}$$

where m_p and U_p can be different for states above and below the Fermi surface. The energies of the states below the Fermi surface should be self-consistently determined with the Brueckner interaction:

$$\varepsilon(k) = \frac{\hbar^2}{2m} k^2 + \sum_{k' < k_F} \langle kk'|G|kk'\rangle \simeq \frac{\hbar^2}{2m^*} k^2 + U. \tag{4.7}$$

There is no consensus on the best treatment of the states above the Fermi surface. One popular prescription is to use free particle energies (Day 1981). This means there will be a gap between particle and hole energies. Other workers use a self-consistency criterion that produces a continuous spectrum (Jeukenne *et al* 1976). We will not be concerned with the details of how equation (4.1) is actually solved. It is an integral equation usually solved by matrix methods in a suitably defined representation.

It is helpful to display the graphical perturbation expansion for the effective interaction to see what processes are included in the theory. The effective interaction is the sum of all perturbation diagrams with four external particle lines, shown as the ellipse in figure 9. The simplest diagram is a single potential interaction between the two particles, shown as the first diagram on the right. The next diagram is the second Born approximation. When successive interactions between the two particles are summed to all orders, the result is the Lippmann-Schwinger equation for the t matrix or the equation for the G matrix.

The single-particle energy effects in the Brueckner theory arise from diagrams such as the third in figure 9. Here one of the interacting particles has a potential interaction with the medium. Diagrams with the medium interaction as a diagonal potential matrix element can be summed to all orders by changing the single-particle energy of the state as given in equation (4.7). In the usual approximation, one neglects the effect of the potential in states above the Fermi surface. The error in doing this is in principle rectified in the next stage of the calculation, where all three-body diagrams are evaluated (Day 1981). The diagrams discussed so far constitute the G matrix interaction of Brueckner theory. The fourth diagram in figure 9 is another medium correction that we will consider shortly.

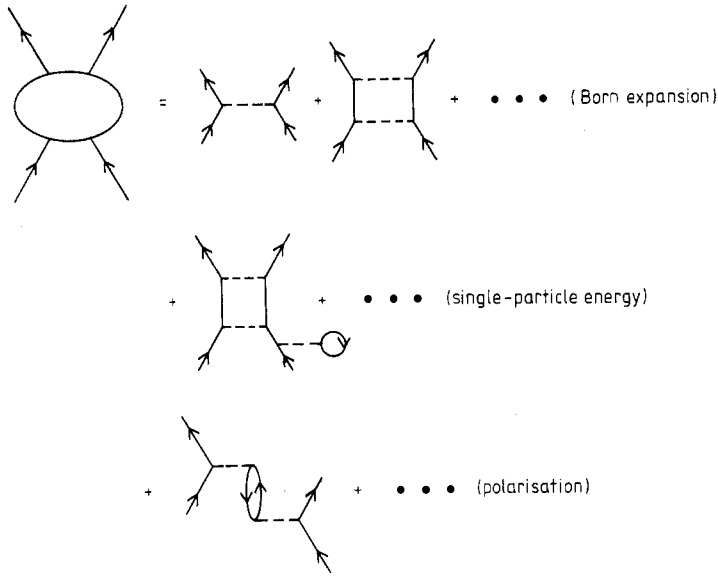

Figure 9. Graphical representation of the different contributions to the G matrix interaction discussed in § 4.2.

4.2. Effective G matrix interactions

The G matrix approaches the free t matrix for high-energy nucleons, but the medium has a dramatic effect on the interaction at lower energies. In particular, the interaction between particle-hole states near the Fermi surface is very different from the free interaction. Since the range of the interaction is small compared with the size of a typical nucleus, it is plausible to neglect the range of the interaction entirely for nuclear structure purposes and to treat it as a contact interaction in the various spin and isospin channels:

$$V_{\rm ph} = (v_0 + v_\sigma \boldsymbol{\sigma}_1 \cdot \boldsymbol{\sigma}_2 + v_\tau \boldsymbol{\tau}_1 \cdot \boldsymbol{\tau}_2 + v_{\sigma\tau} \boldsymbol{\sigma}_1 \cdot \boldsymbol{\sigma}_2 \boldsymbol{\tau}_1 \cdot \boldsymbol{\tau}_2)\delta(\boldsymbol{r}_1 - \boldsymbol{r}_2). \tag{4.8}$$

The values of the v_τ and $v_{\sigma\tau}$ interactions, obtained from different G matrix calculations, are quoted in table 2. They have been determined in the so-called Landau limit and represent the low-frequency long-wavelength interactions between particles moving close to the Fermi surface. If there were a close correspondence between the free interaction and the interaction in the medium, the v in the above equation would be equal to the corresponding t matrix elements at $q = 0$ shown in figure 1. The values of the $v_{\sigma\tau}$ interaction are all in the range 180–220 MeV fm^3. The free t matrix is around 150 MeV fm^3, so the medium effects have only a mild influence on $v_{\sigma\tau}$. Also the values obtained in various G matrix calculations are close to each other, which gives confidence in the resulting interaction. The situation is not so satisfactory for the v_τ interaction. Here the t matrix is strongly energy dependent, and the v_τ values obtained from Brueckner calculations show considerable variation. We shall see in § 4.4 that the empirical interaction, i.e. the interaction required by the empirical spectroscopy, is different from all of these values. Although not directly relevant to the charge exchange interaction, we should also mention that the isoscalar interaction v_0 comes out quite poorly in Brueckner theory.

Table 2. $\sigma\tau$ and τ interactions (MeV fm^3) in the Landau limit.

$v_{\sigma\tau}$	v_τ	Potential source	Reference
From G matrix			
176	68	Hamada-Johnston (1962)	Bertsch *et al* (1977)
217	151	Reid (1968)	Bertsch *et al* (1977)
197	68	Reid (1968)	Bäckmann *et al* (1979)
186	79	Bonn	Dickhoff (1983)
220	85-124	Bonn	Nakayama *et al* (1984)
Empirical values			
150	—	Free t matrix	Figure 1
147 ± 20	190 ± 30	(p, p′) scattering	Austin (1980)
	142	Optical potential	See text
200-240		Gamow-Teller resonance	Bertsch *et al* (1981)
	250-300	Isospin excitations	Bertsch (1983)

4.3. Medium polarisation and the Landau parametrisation

The Brueckner theory is an essential ingredient to derive an effective interaction from a nucleon-nucleon potential, but it is not sufficient. Each particle polarises the medium around it and the polarisation field provides an important part of the total interaction. This is similar to the interaction between electrons in an electron gas. There the polarisation changes the effective interaction from the Coulomb field to a screened Coulomb field. The perturbation diagrams associated with the medium polarisation start with the fourth diagram in figure 9.

The polarisability of the medium is most conveniently discussed in the dimensionless parametrisation of Landau. Here we consider the low-frequency long-wavelength limit of the polarisation of a Fermi gas, induced by a particle just outside the Fermi surface (see e.g. Abrikosov and Khalatnikov 1959). A good measure of the polarisation—or the strength of the interaction V between the particle and particles in the Fermi gas—is the induced density. Landau's original discussion was based on the Boltzmann equation, but a quantal treatment yields exactly the same expression. The momentum transfer to particle-hole excitations is small in the long-wavelength limit. The sum over occupied states can therefore be approximated by an integral over the Fermi surface, and the induced density is

$$\delta n = \int \frac{d\Omega_k}{4\pi} \frac{dN}{d\varepsilon_F} \boldsymbol{q} \cdot \boldsymbol{\nabla}_k \varepsilon(k) \frac{V}{\varepsilon(\boldsymbol{q}+\boldsymbol{k}) - \varepsilon(k)}. \tag{4.9}$$

Here $dN/d\varepsilon_F$ is the density of states at the Fermi surface. The particle inducing the polarisation is also near the Fermi surface, so the only dependence of the interaction on the particle is through the angle θ between the momentum vector of the external particle and a particle in the medium. For $q \to 0$ the energy denominator cancels the factor $\boldsymbol{q} \cdot \boldsymbol{\nabla}_k \varepsilon(k)$ in the numerator and we obtain the expression

$$\delta n = \int \frac{d\Omega}{4\pi} F(\theta) \tag{4.10}$$

where

$$F(\theta) = \frac{dN}{d\varepsilon_F} V(\theta). \tag{4.11}$$

Note that $F(\theta)$ is dimensionless. The Landau parameters are the coefficients in the expansion on Legendre polynomials:

$$F(\theta)=\sum_l F_l P_l(\cos\theta) \tag{4.12}$$

i.e.

$$F_l=(2l+1)\int \frac{d\Omega}{4\pi} P_l(\cos\theta)\frac{dN}{d\varepsilon_F} V(\theta). \tag{4.13}$$

The density of states at the Fermi surface is

$$\frac{dN}{d\varepsilon_F}=\frac{g}{2\pi^2}\frac{mk_F}{\hbar^2} \tag{4.14}$$

where g is the degeneracy of states. Unfortunately, there are two conventions in nuclear physics for choosing the degeneracy factor g. Speth and co-workers use the spin degeneracy, $g=2$. Here we shall use the spin-isospin degeneracy, $g=4$. Then the Landau representation measures the strength of the interaction in units of $d\varepsilon_F/dN=153$ MeV fm^3.

The functional form of the screening can be derived from the RPA formalism discussed in § 5.2. A residual interaction among particle-hole states near the Fermi surface will modify the independent particle response by the factor $(1-v\Pi^{(0)})^{-1}$. In the Landau limit ($\omega\to 0$, $q\to 0$) this factor becomes $(1+F_0)^{-1}$. The importance of the medium polarisation can be assessed from the magnitude of the Landau parameter F_0. The system becomes unstable with respect to density fluctuations if F_0 is less than -1. If F_0 is of order -1 or greater, the polarisation field substantially screens the free interaction. It is clear that the polarisation effects must be very large in the isoscalar channel. The Brueckner interaction has a magnitude of the order of -150 to -300 MeV fm^3, so the medium would be unstable in their absence.

Babu and Brown (1973) have proposed a simple model to estimate the effects of medium polarisation. Essentially, the interaction is assumed to be independent of all momenta, i.e. a delta function. This allows the polarisation graph to be calculated in terms of the Lindhard function. The only subtle point is the spin and isospin coupling, which requires the same linear combinations of spin and isospin amplitudes as was required to express the interaction in particle-particle spin coupling. Recent calculations of medium polarisation have been reported by Dickhoff *et al* (1983) and Nakayama (1985). The polarisation mainly affects the isoscalar channel, reducing the strong attraction. There is a mild repulsive effect on the $v_{\sigma\tau}$ interaction, and virtually no effect on the v_τ interaction.

4.4. Empirical interactions

An interaction can be determined empirically in several ways. The magnitude of the inelastic scattering cross section fixes the strength of the interaction between projectile and target nucleons if the target transition densities and the distorted projectile wavefunctions are known. This method is not reliable for obtaining absolute interaction strengths because of uncertainties in the optical potential. Relative interaction strengths can be obtained with much less ambiguity from this source by comparing cross sections with states of different character in the same nucleus. The relative magnitude of $v_{\sigma\tau}$ and v_τ can be extracted from the (p, n) cross section on a single target. Nuclei used

for this purpose (e.g. ^{7}Li and ^{13}C) have isolated transitions to the IAS and to some other states having a strong GT matrix element. For low-energy protons, the relative cross sections require the spin interaction to be weaker than the spin-independent interaction, roughly by a factor of $\frac{2}{3}$ (Anderson *et al* 1970). This result contradicts Brueckner theory, which predicts $v_{\sigma\tau}$ to be greater than v_τ, as may be seen from table 2. For higher-energy protons, the interaction approaches the free t matrix. This may be seen from the data on intermediate energy (p, n) interactions shown in figure 2.

Austin (1980) has analysed the absolute strength of the interactions for low-energy proton scattering using optical potentials that are consistent with elastic scattering data. His interaction strengths are quoted in table 2. We see that $v_{\sigma\tau}$ is quite close to the free t matrix. The mild medium corrections to the interaction in this channel disappear a small amount above the Fermi energy. The v_τ interaction is the one causing difficulty; it is much larger than the G matrix results, and it is so rapidly varying in the t matrix that no value can be assigned.

Another empirical method for extracting the v_τ interaction is from the isospin dependence of the single-particle Hamiltonian. It has a potential term $V_1(r)\tau_z(N-Z)/A$, where τ_z is the isospin of the particle. The relationship to the interaction is $V_1 = v_\tau \rho$, assuming that all densities have the same radial dependence. We quote a value in table 2 using this formula, with V_1 obtained from Rapaport *et al* (1979) and $\rho = 0.16\ \text{fm}^{-3}$. This value of v_τ is at the upper end of the range found in the G matrix calculations.

Empirical interactions applicable to nucleons at the Fermi surface can be extracted from the energetics of the IAS and the GT resonance. The theory relating the interaction to the excitation energy is discussed in the next section. For completeness we quote some of the results in table 2. In the spin channel, the energy systematics of the GT resonance require an interaction strength in the range 170–220 MeV fm^3, provided the interaction is fairly short-range; with the range of one-pion exchange it needs to be slightly stronger. Overall, the G matrix gives interactions that are consistent with this. Note, however, that the GT resonance is sensitive mainly to the interaction at small momentum transfers. Information about the interaction at large momentum transfers can be obtained from high spin states or from broad strength distributions, but this part of the interaction is not as well determined.

The v_τ interaction extracted from structure energies is stronger than $v_{\sigma\tau}$, as was found in low-energy proton scattering. Again, the Brueckner theory fails in accounting for this interaction.

5. Nuclear structure

In this section we shall review the theoretical techniques used to interpret the nuclear structure aspects of the charge exchange reactions. As we saw in § 3, the DWIA factors the reaction amplitude into a projectile-dependent part and a nuclear transition density. For our purpose, the densities of interest are matrix elements of the charge-changing operators

$$\boldsymbol{\rho}_{\sigma\tau} = \sum_i \boldsymbol{\sigma}_i \tau_\pm \delta(\boldsymbol{r} - \boldsymbol{r}_i) \qquad \boldsymbol{\rho}_\tau = \sum_i \tau_\pm \delta(\boldsymbol{r} - \boldsymbol{r}_i). \tag{5.1}$$

Nuclear structure theory is founded on the description of the nuclear wavefunction by one or more Slater determinants of single-particle orbitals. The orbitals in turn are

defined as eigenstates of a static single-particle Hamiltonian. Useful theory can be done at different levels of sophistication. At the highest level, a large multi-particle configuration space is defined in the shell model representation, along with a model Hamiltonian that includes single-particle energies and residual interactions. The Hamiltonian is diagonalised to produce predictions for matrix elements between all the states. This approach is highly successful when the shell model space is small enough to allow a complete diagonalisation (Wildenthal 1984). The space restriction effectively limits the method to nuclei lighter than $A = 40$ or to nuclei at closed shells. It is the only practical way to get accurate predictions when the ground state is strongly mixed among the shell model configurations.

If the ground state can be reasonably approximated by a single Slater determinant, mean field theory provides an excellent description of the transitions and one that is not limited by the size of the shell model configuration space. When ground state correlations are completely negligible, the Tamm-Dancoff approximation (TDA) is applicable. Some ground state correlations can be included in the mean field description with the random phase approximation (RPA). In either case, the main object of the theory is not the transition matrix elements to individual states, but rather the response function. This is defined for an arbitrary operator O by

$$S(E) = \sum_{\mathrm{f}} |\langle \mathrm{f}|O|\mathrm{i}\rangle|^2 \delta(E_{\mathrm{f}} - E_{\mathrm{i}} - E). \tag{5.2}$$

Here i and f label initial and final states. In mean field theory the only final states in the space are states with one-particle one-hole character. Mostly, one does not attempt to make a very detailed description of $S(E)$; rather one characterises its major features—the total strength, the position of major peaks and the widths of those peaks. The RPA works very well for determining the position of major peaks and their strengths, but it cannot account for the width when the peak is in a region of high level density.

At a very coarse level, some information about the response can be obtained from sum rules. They provide a powerful technique for evaluating the total strength and an average energy by closed formulae. We shall now describe these various theoretical tools in order of increasing complexity, starting with the sum rules.

5.1. Sum rules

The key sum rules of the charge exchange excitation are based on the commutator of the isospin operators:

$$[t_+, t_-] = 2t_z. \tag{5.3}$$

Here we define the operators by $t_\pm = t_x \pm \mathrm{i}t_y$ with cartesian operators having eigenvalues $\pm\frac{1}{2}$. Equation (5.3) can be applied directly to the spin-independent excitations. We evaluate both sides of this equation in the initial state and insert a complete set of final states between the operators on the left-hand side. The result is

$$\langle \psi_{\mathrm{i}}|t_+t_- - t_-t_+|\psi_{\mathrm{i}}\rangle = \sum_{\mathrm{f}} |\langle \psi_{\mathrm{f}}|t_-|\psi_{\mathrm{i}}\rangle|^2 - \sum_{\mathrm{f}} |\langle \psi_{\mathrm{f}}|t_+|\psi_{\mathrm{i}}\rangle|^2 = 2\langle \psi_{\mathrm{i}}|t_z|\psi_{\mathrm{i}}\rangle. \tag{5.4}$$

Because the initial state is close to an isospin eigenstate, the result is trivial; the initial state typically has isospin $T_z = (N - Z)/2$, so the second term vanishes and we have

$$\sum_{\mathrm{f}} |\langle \psi_{\mathrm{f}}|t_-|\psi_{\mathrm{i}}\rangle|^2 = N - Z. \tag{5.5}$$

The result is not so trivial for the GT operator, which we define in terms of the Pauli spin matrices σ_μ as

$$\beta_\mu^\pm = \sum_i \sigma_\mu(i) t_\pm(i). \tag{5.6}$$

The corresponding commutator relation is

$$\sum_{\mu=1}^{3} [\beta_\mu^+, \beta_\mu^-] = 6t_z. \tag{5.7}$$

The sum rule based on this relation was first applied to spectroscopic studies by Gaarde *et al* (1980). Evaluating this expression in the ground state gives

$$S_{\beta^-} - S_{\beta^+} = \sum_{f\mu} |\langle \psi_f | \beta_\mu^- | \psi_i \rangle|^2 - \sum_{f\mu} |\langle \psi_f | \beta_\mu^+ | \psi_i \rangle|^2 = 3(N-Z). \tag{5.8}$$

Thus the difference in total strength for β^- and β^+ decay is fixed by this sum rule. The β^+ strength function is quite weak, although not forbidden by isospin conservation like the t_+ strength, so for practical purposes the sum rule can be viewed as a close lower bound on the β^- strength. In the next section we shall use this bound, calling it the sum rule bound.

These sum rules have a significance extending outside nuclear physics to the QCD theory of hadrons. The current algebra theory of hadronic processes is fundamentally based on the extension of these operators to the four-component Dirac operators. Doubling the dimensionality of the operators has no effect on the commutators themselves. But the operators are interpreted to act on the fundamental quark fields. Adler and Weissberger (see Adler and Dashen 1968) applied the analogue of equation (5.8) involving the axial vector current, choosing ψ_i to be a nucleon and ψ_f to be either a nucleon or a nucleon plus pion state. They were able to estimate the matrix element to the nucleon plus pion state and show consistency with the sum rule, with a nucleon matrix element close to the empirical value

$$g_A = \langle p | \beta_{\text{quark}}^- | n \rangle = 1.26. \tag{5.9}$$

The matrix element is larger than one because the $N+\pi$ states have a preponderance of β^+ strength. For our purposes we will only use the sum rule at the level of nuclear physics, with $\langle p|\beta^-|n\rangle = 1$. A failure of the nuclear sum rule would then signal that the mesonic effects behave differently within the nucleus than they do for free nucleons.

5.2. Response functions in mean field theory

The theory of the response starts from the independent particle model. First the single-particle Hamiltonian is defined, and its eigenfunctions ϕ_α and eigenvalues ε_α are calculated. The independent particle response to a single-particle operator O is then obtained from the equation

$$S(E) = \sum_{\alpha\alpha'} n_\alpha (1 - n_{\alpha'}) |\langle \phi_{\alpha'} | O | \phi_\alpha \rangle|^2 \delta(E + \varepsilon_\alpha - \varepsilon_{\alpha'}). \tag{5.10}$$

Here $n_\alpha = 0$ or 1 is the occupancy of a given orbit α.

The effective Hamiltonian also contains a residual interaction which has major effects on the response, but the independent particle model still provides a useful orientation. For smooth operators, there are major concentrations of strength that are identified with specific transitions between shells. A simple illustration is the closed

shell nucleus ^{90}Zr. It has all shells filled up to the g-orbit. Within the g-orbit, only the $g_{9/2}$ neutron orbit is occupied. The GT and the isobaric analogue transitions are schematically illustrated in figure 10. The strength function for the operator t_- will have a single peak at an excitation energy of $E = \varepsilon^{p}_{9/2} - \varepsilon^{n}_{9/2}$ in the independent particle model. The GT operator can make transitions from $g^{n}_{9/2}$ to $g^{p}_{9/2}$ or $g^{p}_{7/2}$, giving two peaks in the spectrum.

Calculations in the independent particle model require specification of the single-particle Hamiltonian. This consists of a charge-independent part, which we write as

$$H_{sp} = T + U(r) + V_{ls}(r)\boldsymbol{l}\cdot\boldsymbol{s} \tag{5.11}$$

together with a part that depends on whether the particle is a proton or a neutron. Here T is the kinetic energy operator, $U(r)$ is a local potential and $V_{ls}(r)$ is the spin-orbit field. The empirical phenomenology of the shell model constrains these potentials quite strongly; in fact, better than they can be determined from first principles and Brueckner theory. For example, the spin-orbit splitting of high l orbitals near the Fermi level is of the order of 5-6 MeV, and the $V_{ls}(r)$ must reproduce this. One aspect of the Hamiltonian that is not so certain concerns the non-locality in the potential. The influence of this can be parametrised by using an effective mass different from the free nucleon mass in T. The empirical spectroscopy near the Fermi level is quite compatible with an effective mass of one (in units of the nucleon mass). On the other hand, the optical potential for nucleons in the continuum, and the electromagnetic response at high momentum transfers, favour an effective mass in the range 0.8-0.9. The Brueckner theory predicts an effective mass smaller than one; for example, Negele and Vautherin (1972) calculate $m^* = 0.6$. One of the most noticeable features of mean field theories based on Dirac potentials is that they also predict effective masses much smaller than one. For the GT and the IAS transitions, the effective mass uncertainty plays no direct role because the momentum of the particles is not changed. However, the excitation energy of transitions requiring a finite momentum transfer, such as $L = 1$ transitions, will depend on the assumptions about the effective mass.

It is important to include the residual interaction for a quantitative theory of the response. The mean field theory can be constructed very conveniently by generalising the response to a complex function of densities at two points, namely the independent particle polarisation operator

$$\Pi^{(0)}(E, \boldsymbol{r}, \boldsymbol{r}') = \sum_{\alpha\alpha'}{}' n_\alpha(1-n_{\alpha'}) \frac{\phi^*_\alpha(\boldsymbol{r})\phi_{\alpha'}(\boldsymbol{r})\phi^*_{\alpha'}(\boldsymbol{r}')\phi_\alpha(\boldsymbol{r}')}{E + i\eta - \varepsilon_{\alpha'} + \varepsilon_\alpha}. \tag{5.12}$$

This is actually the polarisation operator used in the Tamm-Dancoff approximation

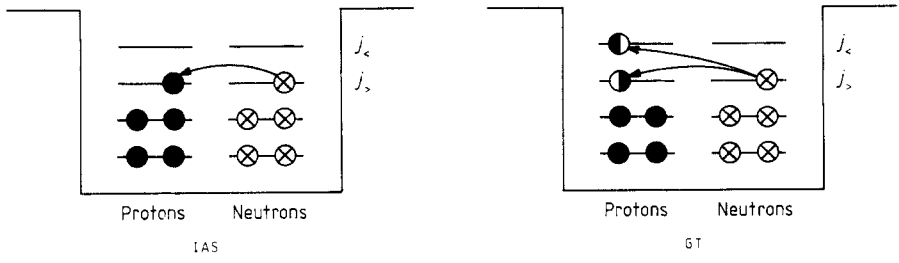

Figure 10. Schematic shell model picture of isobaric analogue (IAS) and Gamow-Teller (GT) transitions. The τ operator replaces a neutron by a proton in the same orbit. The $\sigma\tau$ operator can place the proton in both the $j_>$ and the $j_<$ orbits.

(TDA). The retarded polarisation operator used to calculate the RPA response contains in addition the poles $-1/(E+i\eta+\varepsilon_{\alpha'}-\varepsilon_{\alpha})$; see e.g. Bertsch (1983). In both approximations the polarisation operator that includes the effect of a residual interaction $v(r, r')$ is

$$\Pi(E, \boldsymbol{r}, \boldsymbol{r}') = \Pi^{(0)}(1 - v\Pi^{(0)})^{-1}. \tag{5.13}$$

This equation is to be understood as an operator equation, i.e. the operators are expanded in some basis and the operations on the right-hand side are performed as matrix operations. Since the polarisation operator involves only the local densities, non-local operators such as the exchange interaction cannot be incorporated in (5.13) exactly. It is common to use a zero-range approximation to the exchange interactions. Otherwise, the residual interaction must be treated by a matrix diagonalisation in the space of configurations. The response to an operator O is calculated from the polarisation operator by the integral

$$S(E) = -\frac{1}{\pi}\,\mathrm{Im}\int \mathrm{d}\boldsymbol{r}\,\mathrm{d}\boldsymbol{r}'\,O^{+}(\boldsymbol{r})\Pi(E, \boldsymbol{r}, \boldsymbol{r}')O(\boldsymbol{r}'). \tag{5.14}$$

The simplest theory including residual interactions is the TDA, which is given by equations (5.12)-(5.14) as written. The TDA theory respects the sum rules (5.5) and (5.8). It also has the property that the average excitation energy is given by the commutation expression

$$\langle E\rangle = \int_0^{\infty} \mathrm{d}E\,E\,S_{\mathrm{TDA}}(E) = \frac{\langle O^{+}[H, O]\rangle}{\langle O^{+}O\rangle}. \tag{5.15}$$

The expectation value is taken in the independent particle wavefunction of the parent state. The operator in (5.15) is evaluated by explicitly summing over intermediate particle-hole states. For the present application, we separate H into charge-dependent and spin-dependent parts together with a scalar Hamiltonian:

$$H = H_{\mathrm{sp}} + \sum_{i<j} v_{\sigma\tau}(\boldsymbol{\sigma}_i\cdot\boldsymbol{\sigma}_j)(\boldsymbol{\tau}_i\cdot\boldsymbol{\tau}_j) + v_{\tau}\boldsymbol{\tau}_i\cdot\boldsymbol{\tau}_j + \frac{e^2(1-\tau_{iz})(1-\tau_{jz})}{4|\boldsymbol{r}_i-\boldsymbol{r}_j|}. \tag{5.16}$$

We can then make the corresponding separation of the mean excitation energy

$$\langle E\rangle = \Delta E_{\mathrm{orbit}} + \Delta E_{ls} + \Delta E_{\sigma\tau} + \Delta E_{\tau} + \Delta E_{C}. \tag{5.17}$$

The energetics of the IAS and the GT state can be most conveniently discussed by assuming that all of the t_- and the β^- strengths are concentrated in single states. In the TDA the resulting energy will be just the mean value computed in (5.15). The normalised coherent states are defined by

$$|\mathrm{IAS}\rangle = \sum_{\mathrm{ph}} |\mathrm{ph}\rangle\langle \mathrm{p}|t_-|\mathrm{h}\rangle/(N-Z)^{1/2} \tag{5.18}$$

$$|\mathrm{GT}\rangle_{\mu} = \sum_{\mathrm{ph}} |\mathrm{ph}\rangle\langle \mathrm{p}|\beta^-_{\mu}|\mathrm{h}\rangle/(\tfrac{1}{3}S_{\beta^-})^{1/2} \tag{5.19}$$

where the sum is over all particle-hole states.

The theory of $\langle E\rangle$ is particularly simple for the Fermi transition operator t_-, since it commutes to an excellent approximation with all of the terms in H that conserve isospin. The $v_{\tau}\boldsymbol{\tau}_1\cdot\boldsymbol{\tau}_2$ term in the Hamiltonian contributes both to the single-particle energies and to the residual interaction in the IAS, but these contributions necessarily cancel. All terms in the Hamiltonian (5.16) except the Coulomb conserve isospin, so

the energy expectation (5.15) depends only on that term. Evaluation of the commutator with $O = t_-$ yields

$$\langle E_{\mathrm{IAS}}\rangle = e^2 \int \mathrm{d}\boldsymbol{r}\,\mathrm{d}\boldsymbol{r}'\,\frac{\rho_{\mathrm{p}}(\boldsymbol{r})(\rho_{\mathrm{n}}(\boldsymbol{r}')-\rho_{\mathrm{p}}(\boldsymbol{r}'))}{|\boldsymbol{r}-\boldsymbol{r}'|(N-Z)} \tag{5.20}$$

for the direct part of the interaction. Because isospin is nearly conserved, the strength is very concentrated in a single state or a narrow group of states. Thus (5.20) is the energy of the isobaric analogue state (IAS). The integral may be evaluated using densities obtained from the occupied orbits of the single-particle Hamiltonian. If we require the Hamiltonian to reproduce the charge radius of the nucleus, the predicted energy of the IAS is within a few per cent of the observed analogue state. However, (5.20) does not include the exchange Coulomb interaction. When this and other small effects are included, the theoretical value is off by 7%, which has been a long-standing problem in nuclear structure physics (Nolen and Schiffer 1969).

5.2.1. Energy of the Gamow-Teller resonance. The energetics of the Gamow-Teller strength function are more complicated, because more terms in the Hamiltonian fail to commute. Let us first consider the residual interaction term $v_{\sigma\tau}(\boldsymbol{r}_1-\boldsymbol{r}_2)(\boldsymbol{\sigma}_1\cdot\boldsymbol{\sigma}_2)\times(\boldsymbol{\tau}_1\cdot\boldsymbol{\tau}_2)$. In order to make a non-vanishing expectation value in (5.15), the operators O^+ and O must act on particles 1 and 2. Here $O=\beta^-_\mu$. Using the definition (5.19) of the coherent GT state, the energy shift can be written as the expectation value

$$\Delta E_{\sigma\tau} = \langle \mathrm{GT}|v_{\sigma\tau}(\boldsymbol{\sigma}_1\cdot\boldsymbol{\sigma}_2)(\boldsymbol{\tau}_1\cdot\boldsymbol{\tau}_2)|\mathrm{GT}\rangle. \tag{5.21}$$

We can express this energy shift in terms of the transition density for the GT state,

$$\delta\rho_{\mathrm{GT}} = \langle \mathrm{GT}|\boldsymbol{\rho}|0\rangle = \sum_{\mathrm{ph}} \frac{\langle \mathrm{p}|\beta^-_\mu|h\rangle}{(\frac{1}{3}S_{\beta^-})^{1/2}}\,\phi^*_{\mathrm{p}}\phi_{\mathrm{h}} \tag{5.22}$$

and obtain

$$\Delta E_{\sigma\tau} = 2\int \mathrm{d}\boldsymbol{r}\,\mathrm{d}\boldsymbol{r}'\,\delta\rho_{\mathrm{GT}}(\boldsymbol{r})v_{\sigma\tau}(\boldsymbol{r}-\boldsymbol{r}')\delta\rho_{\mathrm{GT}}(\boldsymbol{r}'). \tag{5.23}$$

The factor of 2 arises from the isospin operator $\boldsymbol{\tau}_1\cdot\boldsymbol{\tau}_2$, which can be decomposed into $2(t_{1+}t_{2-}+t_{1-}t_{2+})+\tau_{1z}\tau_{2z}$. This expression can easily be estimated if we make two assumptions. The first is that the range of the interaction is small compared with the nuclear size. Then it can be approximated by the zero-range form

$$v_{\sigma\tau}(\boldsymbol{r}_1-\boldsymbol{r}_2) = v_{\sigma\tau}\delta(\boldsymbol{r}_1-\boldsymbol{r}_2). \tag{5.24}$$

The second assumption is that the transition density is proportional to the ground state density, $\delta\rho_{\mathrm{GT}}\propto\rho$. Normalising this to the integral

$$\int \mathrm{d}\boldsymbol{r}\,\delta\rho_{\mathrm{GT}} = (\tfrac{1}{3}S_{\beta^-})^{1/2} \tag{5.25}$$

the normalised density is

$$\delta\rho_{\mathrm{GT}} = (\tfrac{1}{3}S_{\beta^-})^{1/2}\,A^{-1}\rho(r). \tag{5.26}$$

The integral (5.23) is now expressed in the form

$$\Delta E_{\sigma\tau} = v_{\sigma\tau}\langle\rho\rangle\,2S_{\beta^-}/3A \tag{5.27}$$

where $\langle\rho\rangle$ is the average magnitude of the density weighted by its radial distribution. This is a quantity that does not vary much from nucleus to nucleus and has the order of magnitude of the nuclear saturation density. Numerical calculation with valence neutron densities obtained from the single-particle Hamiltonian gives the magnitude $\langle\rho\rangle \simeq \frac{3}{4}\rho_0 \simeq 0.12\ \mathrm{fm}^{-3}$.

The effective strength of the residual interaction depends on the product of the integrated strength and the average density:

$$\kappa_{\sigma\tau} = v_{\sigma\tau}\langle\rho\rangle. \tag{5.28}$$

A numerical estimation of $\kappa_{\sigma\tau}$, using a typical value of $v_{\sigma\tau}$ from table 2, is $\kappa_{\sigma\tau} = 200 \times 0.12\ \mathrm{MeV} = 24\ \mathrm{MeV}$.

We next consider the Coulomb and the isovector nuclear single-particle energies. These contribute the same amount in the GT energy as in the IAS; so instead of calculating these terms, we may just add the analogue state energy. However, the IAS has an additional contribution from the residual v_τ interaction, which must then be explicitly subtracted. That contribution may be treated in the same way as the $v_{\sigma\tau}$ residual interaction, defining

$$\kappa_\tau = v_\tau\langle\rho\rangle. \tag{5.29}$$

The one remaining term is the spin-orbit potential. This can vary depending on the specific shells of the valence neutrons, but usually most of the excess neutrons occupy high j valence orbits. In a typical situation in heavy nuclei, the parent nucleus has only the $j_>$ shell filled, while the daughter nucleus has both $j_>$ and $j_<$ empty; or if the daughter nucleus has $j_>$ filled and $j_<$ empty, both shells will be occupied in the parent nucleus. The operator β^- has roughly equal strengths for spin flip as compared to non-spin flip transitions. Since the transitions are half blocked by occupancy factors, the expectation value of the spin-orbit potential will be

$$\Delta E_{ls} = \tfrac{1}{2}(\varepsilon_{j_>} - \varepsilon_{j_<}) \simeq 3\ \mathrm{MeV}. \tag{5.30}$$

A simple formula can now be obtained by assuming that the β^- strength exhausts the sum rule, $S_{\beta^-} = 3(N-Z)$. The mean excitation energy of the GT strength is then given by

$$\langle E_{\mathrm{GT}}\rangle - \langle E_{\mathrm{IAS}}\rangle = \Delta E_{ls} + \frac{\kappa_{\sigma\tau} - \kappa_\tau}{A} 2(N-Z). \tag{5.31}$$

Figure 11 shows the data on the position of the GT resonance compared with the functional form (5.3) (from Nakayama *et al* 1982). For nuclei with small neutron excess, the ΔE_{ls} dominates and the GT state lies above the IAS. For the heaviest nuclei, such as ^{208}Pb, the second term balances the first and the GT state is at the same energy as the IAS. The slope of the line requires that κ_τ be larger than $\kappa_{\sigma\tau}$. This is the reverse of the prediction from Brueckner theory. However, κ_τ is compatible with the empirical interaction deduced from low-energy (p, p′) scattering or from isospin excitations, as given in table 2.

The difference in interaction strength between v_τ and $v_{\sigma\tau}$ is also apparent in the energy of the $L=1$ excitations. The $L=1$ response is not as sharply localised as the $L=0$, as may be seen from figure 8, but it still stands out sufficiently over the background to define a peak position. It is higher in energy than the GT resonance for two reasons. First, the kinetic energy in the Hamiltonian contributes to the sum (5.17) for any excitation that is spatially inhomogeneous. Also, there is less Pauli blocking and more

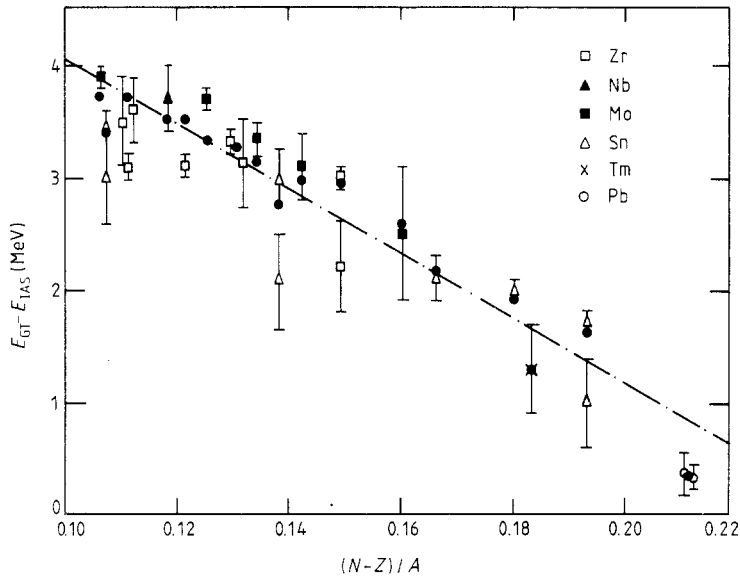

Figure 11. Energy difference of the Gamow-Teller and the isobaric analogue state for different nuclei as a function of the relative neutron excess; the correlation illustrates the functional form of equation (5.30) (from Nakayama *et al* 1982). (Used with the permission of the authors and North-Holland Publishing Company.)

particles participate in the excitation, making a larger contribution to the residual interaction. The position of the $L = 1$ peak, as seen with intermediate-energy proton scattering, is 6.6 MeV in ^{208}Pb and 12.6 MeV in ^{90}Zr, measured with respect to the IAS (Bainum *et al* 1980, Horen *et al* 1981). Charge exchange scattering of 40 MeV protons also shows an $L = 1$ peak, but centred at a 2.5 MeV higher energy (Sterrenburg *et al* 1980). The intermediate-energy proton excites mainly the spin mode, while the lower-energy beam also makes spin-independent excitations. Let us estimate the interaction energy of the scalar dipole mode at about 8 MeV. Then the strength of the $v_{\sigma\tau}$ interaction should be 25% smaller than the v_τ interaction to explain the shift.

5.2.2. Fragmentation of the Gamow-Teller strength. The sum rule treatment is adequate to describe the position of the GT resonance, since the strength function is quite concentrated. However, there are also weak GT transitions at low excitation energies, which are important in beta decay. Explicit calculation of (5.13) with the detailed shell structure of (5.12) is necessary for a more accurate treatment.

One approximation greatly simplifies the calculation. Assume that the individual matrix elements of the residual interaction are proportional to the matrix elements of the GT operator:

$$\langle \alpha\beta^{-1}|v_{\sigma\tau}(\boldsymbol{\sigma}_1 \cdot \boldsymbol{\sigma}_2)(\boldsymbol{\tau}_1 \cdot \boldsymbol{\tau}_2)|\alpha'\beta'^{-1}\rangle = \frac{\kappa_{\sigma\tau}}{A}\langle \alpha|\beta^-|\beta\rangle\langle \alpha'|\beta^-|\beta'\rangle. \tag{5.32}$$

This interaction, of course, reproduces the energy of the GT state and by itself makes the GT an eigenstate of the Hamiltonian H. Equation (5.32) is a useful approximation because the fragmentation of the GT state is more influenced by other terms in the Hamiltonian, such as the single-particle energies, than in the fluctuations of individual particle-hole matrix elements about (5.32). The separability of this interaction allows

(5.13) to be solved as an algebraic equation. This technique has been exploited by Klapdor (1981) to find a semi-phenomenological description of beta decay rates over the entire periodic table.

Two aspects of the strength fragmentation are fairly easy to understand without detailed calculations. Part of the fragmentation is associated with the conflict between the spin-orbit field and the residual interaction. The $v_{\sigma\tau}$ interaction (5.32) is diagonal in the GT state (5.19), but the spin-orbit field is not. The off-diagonal matrix elements of $V_{ls}\boldsymbol{l}\cdot\boldsymbol{s}$ are then responsible for the fragmentation. These matrix elements can be estimated at about half the spin-orbit splitting, so in perturbation theory a quarter of the strength is transferred to the lower states. This may be seen in figure 12, showing the GT strength in ^{208}Pb for the independent particle model and with a residual interaction included (Sagawa and Van Gai 1982). The thin vertical lines are the transition strengths of the individual particle-hole configurations, while the broader bars are the result of diagonalising a residual interaction. The most obvious effect of the interaction is to shift most of the strength to a single state at high excitation, but a secondary peak may also be seen having about a quarter of the strength of the upper state. Empirically, one observes the two pieces of the GT strength in light and medium-heavy nuclei, and the relative strength agrees with theory (Bertsch *et al* 1981). However, in heavy nuclei the observed strength is a single continuous peak extending to lower energies. Here there must be mechanisms beyond mean field theory that are important in spreading the strength.

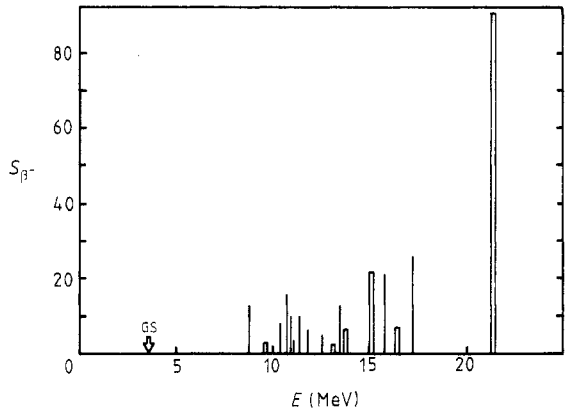

Figure 12. Gamow-Teller transition strength for (p, n) reactions on ^{208}Pb; the thin vertical lines represent the independent particle response and the broader bars are the collective strength obtained in the random phase approximation (from Sagawa and Van Gai 1982). (Used with the permission of the authors and North-Holland Publishing Company.)

Another way to view the fragmentation in mean field theory is to start from the independent particle picture, which may have transitions between orbits near the Fermi level. Not all of the strength of these low-energy transitions is taken away by the GT state. Equations (5.12) and (5.13) may be used to estimate the remainder by treating $(1-v\Pi^{(0)}(E))^{-1}$ as a number that renormalises the strength. The $\Pi^{(0)}(E)$ varies with energy as $1/(E-E_{\rm IP})$, where $E_{\rm IP}$ is the excitation energy in the independent particle model. To have the GT state at $E_{\rm GT}$ requires $1-v\Pi^{(0)}(E_{\rm GT})=0$. Then

$$(1-v\Pi^{(0)}(E))^{-1}=\frac{E-E_{\rm IP}}{E-E_{\rm GT}}. \tag{5.33}$$

Typically $E_{IP} - E = 3$ MeV and $E_{GT} - E = 10$ MeV, so the strength for the low-lying transitions is reduced by a factor of three. This renormalisation in fact was the main empirical evidence available when Ikeda *et al* (1963) first proposed that the GT strength might be concentrated in a state at high excitation.

5.2.3. RPA and β^+ transitions. The full RPA treatment is required for the mean field theory of the β^+ transitions. This is because the correlations that suppress the low-energy transition strength are not contained in the particle-hole spectrum of the β^+ operator. The correlations are associated with the GT resonance, which is only reached by the β^- operator. The mean field theory using the full polarisation operator includes both kinds of excitations. The β^+ spectrum can be viewed as an extension of the β^- spectrum to negative energies in RPA theory. The suppression of strength will not be quite as large in the β^+ case because the energy differences in (5.33) are larger. For example, in the nucleus ^{60}Ni the RPA calculations of Auerbach *et al* (1982) predict a factor of 2 suppression with respect to the independent particle model.

As mentioned earlier, the mean field theory is not reliable for open shell nuclei, because of the strong configuration mixing. Some of the correlation effects can be incorporated into the theory by using a quasi-particle basis to treat pairing correlations (Kisslinger and Sorensen 1963). The pairing suppresses the quasi-particle transitions, which would be the lowest in the spectrum, but the total β^+ and β^- strengths are not much affected. A systematic study of the β^+ strength in open shell nuclei was recently made by Cha (1983). The RPA correlations suppress the low transitions by a factor of 3 to 10 with respect to the independent quasi-particle model. However, observed transition strengths are even more suppressed, typically by an additional factor of 4. Because only the very lowest states can be seen by β decay, the empirical knowledge of the β^+ strength function is not sufficient to tell what is wrong with the quasi-particle RPA theory.

5.3. Hamiltonian diagonalisation

Wavefunctions constructed from Hamiltonian diagonalisation in a multi-particle configuration space can provide accurate and detailed information about the response, much superior to what can be achieved with other methods. We shall not describe how the calculations are performed. The interested reader is referred to the review article by Wildenthal (1984) for details. Unfortunately, the method is only reliable when the configuration space covers the complete set of configurations in the active major shell. Excepting nuclei near shell closures, this limits the applicability to the ranges $5 < A < 14$, where the p-shell is active, and $17 < A < 39$, where the sd-shell is active. For p-shell nuclei, the first study based on complete diagonalisation of the major shell was the work of Cohen and Kurath (1965), and their wavefunctions still serve as a useful theoretical reference. With only interactions among the $p_{3/2}$ and $p_{1/2}$ orbitals to be considered, the energies of known states provide enough information to determine the Hamiltonian, at least its central part.

The general characteristics of the spin-isospin response, namely the suppression and the shift to higher energy as compared with the independent particle shell model, may be easily seen in the p-shell results. The nucleus ^{12}C, located near the middle of the p-shell, provides a good example. The strongest transition for the $\sigma\tau$ operator is the 1^+ ground state of ^{12}N, which is the isobaric analogue of a state at 15.1 MeV in ^{12}C. In the independent particle shell model, the ground states of ^{12}C and ^{12}N have

configurations $(p_{3/2})^8$ and $(p_{3/2})^7 p_{1/2}$ respectively. The excitation energy of this state is nearly twice as large as it is in the independent particle picture, where the energy would be due entirely to the spin-orbit splitting between the $p_{1/2}$ and the $p_{3/2}$ shells. The transition strength of the $\sigma\tau$ operator, as measured in β decay, is 1.00, to be compared with the value 4 that would be obtained from the independent particle picture. Thus the suppression relative to the shell model is a factor of 4. This is in good agreement with the predicted suppression from the Cohen and Kurath wavefunctions, which give values ranging from 0.92 to 0.97. The physics behind this suppression is quite simple. The two-particle interaction in the Hamiltonian tends to pair off the spins in the ^{12}N ground state, preventing the $\sigma\tau$ operator from making transitions.

Another interesting p-shell transition is the ^{14}C to ^{14}N transition, illustrating that apparently allowed transitions can be nearly totally suppressed by configuration mixing. The GT β decay of ^{14}C to the ground state of ^{14}N is hindered with respect to the pure configuration transition from $(p_{1/2})^2$ to $(p_{1/2})^2$ by a factor of 10^5. In this case the Cohen and Kurath wavefunction only predicts a hindrance by a factor of 10, which comes about by an interference of amplitudes from different configurations. When the cancellation is nearly complete the hindrance factor is very sensitive to the details of the Hamiltonian, such as the tensor interaction (Zamick 1966), and an accurate calculation is not possible.

The sd-shell has a much more complex spectroscopy than the p-shell, with the dimensionality of configurations ranging up to several thousands in the middle of the shell. Nevertheless, it has proved possible to carry out the same program as for the p-shell. Wildenthal and his collaborators determine a two-particle Hamiltonian by fitting energy level data, and then use the associated wavefunctions to predict all interesting observables. The results for the $\sigma\tau$ operator are given by Brown and Wildenthal (1985). The accuracy of the Hamiltonian model is illustrated in figure 13, showing the computed $\sigma\tau$ strengths compared with the strengths measured in β decay. The units on the graph are chosen so that the points would fall on the diagonal for perfect agreement. There is a very strong correlation between the predicted and the measured values. However, the best fit requires the $\sigma\tau$ operator to be renormalised by an overall factor of 0.77 in amplitude or 0.6 in intensity. The scatter seen in figure 13 is considerably reduced if the transition strengths are summed over observed final states. This is to be expected because the Hamiltonian is better at describing the overall distribution of strength than its apportionment among nearby levels.

The reaction ^{26}Mg(p, n)^{26}Al illustrates a rather complex spectroscopy of the $\sigma\tau$ operator that is nevertheless well described by the multi-configuration shell model. The cross section for this reaction was measured by Madey *et al* (1987) and compared with theory. Many states are excited and the relative strengths of nearby configurations have no significance, so the strength distributions were artificially smoothed. The result is shown in figure 14. There are several concentrations of strength in the spectrum. The peak at low excitation energies is associated with transitions leaving the particles in the same shells, and the peak at high excitations is dominated by transitions from $d_{5/2}$ to $d_{3/2}$ orbits. The relative strengths and energy distributions agree very well with theory, but only the calculated strength function is renormalised by the factor 0.6.

The Hamiltonian diagonalisations in the sd-shell can also be used to study aspects of the strength functions not directly observable. Thus the β^+ strength function is poorly known compared with our extensive knowledge of the β^- from the (p, n) reaction. As discussed earlier, one would like to know the total β^+ strength, in particular the suppression in comparison to the independent particle strength. The sd-shell

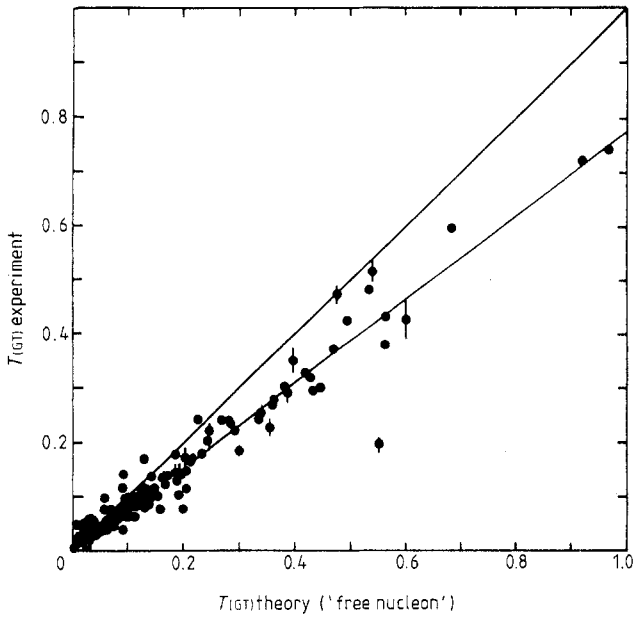

Figure 13. Comparison of experimental Gamow-Teller (GT) matrix elements for sd-shell nuclei with the predictions from diagonalisation of the multi-configuration shell model Hamiltonian (from Brown and Wildenthal 1985). The matrix elements are normalised so that one corresponds to the maximum permitted by the shell model space. For perfect agreement the points should lie on the diagonal line. They actually cluster around a line with a slope of 0.77, showing the overall quenching of the spectroscopic GT strength. (Used with the permission of the authors and Academic Press.)

diagonalisation provides some predictions here; for example, in the nucleus ^{22}Ne the β^+ strength is suppressed by a factor of 10 in comparison with the pure configuration (Brown *et al* 1981). Evidently, each proton is very likely to be spin-paired with some neutron in the configuration-mixed ground state.

Beyond the sd-shell, the multi-configuration calculations have necessarily been incomplete. Bloom and Fuller (1985) have calculated β^+ strength functions in the fp-shell in as large a basis as was feasible. These transitions are particularly interesting because of their role in stellar collapse. The core of a supernova precursor is rich in fp-shell nuclei such as iron. During the collapse, inverse β decays occur, eventually leading to a neutron star, unless a black hole is formed. The detailed dynamics of the collapse process is sensitive to the inverse β decay rates (Bethe *et al* 1979).

Bloom and Fuller were unable to perform complete shell model diagonalisations in the mid fp-shell, but they could determine the structure of the strength functions associated with simple initial configurations. They found that most of the strength occurs at low excitation energies in the residual nucleus, in the range of 2-4 MeV above the ground state. Unfortunately, the calculations give no information about the total strength, because the simple initial configurations do not allow spin pairing to develop.

Muto (1986) has made a similar study limited to nuclei with $N = 28$. The initial configurations start from pure $f_{7/2}$ configurations, but Muto allows up to two-particle excitations out of the $f_{7/2}$ shell. His results confirm the previous findings that the strength is concentrated within a few MeV of the ground state. Because of his larger

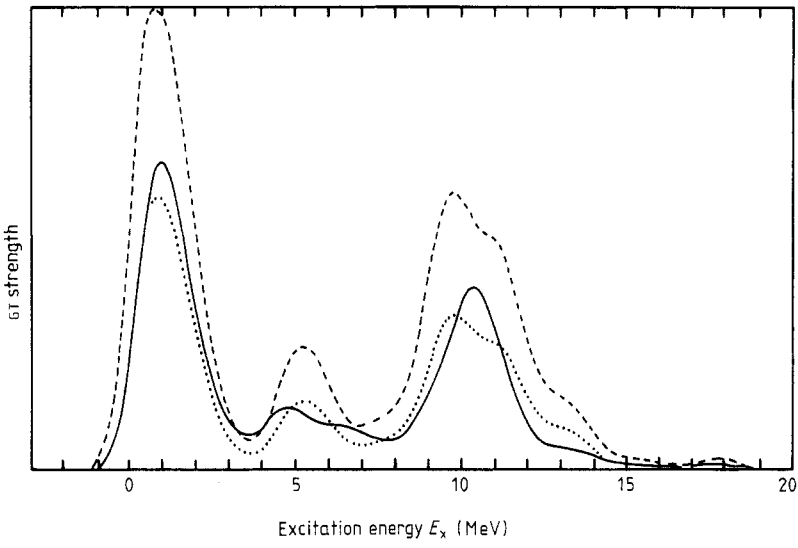

Figure 14. The excitation function for the Gamow-Teller (GT) operator in ^{26}Mg (from Madey *et al* 1987). The full curve is the strength as measured in the forward-angle (p, n) reaction using 134 MeV protons. The broken curve is the prediction of the multi-configuration shell model. The discrete states in both spectra have been artificially smeared to make it easier to see the overall behaviour of the strength function. The dotted curve is the theoretical curve renormalised by a factor of 0.57. (Used with the permission of the authors prior to publication.)

configuration space, he is able to see quenching of the total strength. He finds that the total strength is reduced by a factor of 0.5–0.6 compared with the pure configuration. Thus, with an additional renormalisation of 0.6 that must arise from outside effects in the major shell, a quenching to 0.3–0.4 of the pure configuration may be expected.

6. Gamow–Teller strength function

6.1. Measured Gamow–Teller strength

Initial measurements of the β^- strength in (p, n) reactions determined values for the total strength that were a fraction of the sum rule bound. For example, Gaarde *et al* (1981) compared their measured cross sections with an absolute DWIA calculation based on the Love and Franey *t* matrix interaction and the optical potential of Nadasen *et al.* The measured cross section in the peaks of the forward-angle spectra was only 30% of the sum rule prediction from the DWIA analysis. However, it is clear that the DWIA theory is not reliable enough to be used in an absolute sense. A much safer way to analyse the data is to normalise the (p, n) reaction cross sections to known β transition rates. Gamow-Teller β decays with large transition rates are only found in the lighter nuclei, so the renormalisation can be done very reliably there. As we saw in figure 14, the strength to higher states corresponds very well with the shell model prediction if the same renormalisation is applied to the entire spectrum. There are no additional peaks in the spectrum to account for the missing strength. Using this kind of analysis, Goodman and Bloom (1984) concluded that 50–60% of the sum was present for nuclei in the range $A = 13$–90.

In heavier nuclei there is no possibility of resolving individual states, and the analysis is based on spectra that appear continuous. In the first analyses, the cross section for the main GT peak was extracted assuming a smooth background underneath the peak. The background was drawn to join onto the yield at higher excitation energies, where the spectrum is quite flat. This procedure was criticised by Osterfeld (1982), who calculated the inclusive (p, n) cross section in the DWIA, including many multipolarities of transitions in the independent particle shell model. He found that the higher multipoles, notably $L = 1$, could explain most of the forward-angle yields at higher excitation energies, above the GT peak. However, these multipoles gave a negligible contribution at the peak energy and below, as shown in figure 15. There is therefore no justification for extending the background down to the GT peak region. It was then verified from the experimental angular distribution that essentially all of the cross section in the peak region has an $L = 0$ character. When the dubious background subtraction is omitted, the sum for heavy nuclei falls in the range of 50–60% of the bound. This is illustrated in figure 16 (from Gaarde 1985).

The next obvious place to look for missing GT strength is in the continuum, above the peak. This is not an easy task from an experimental point of view, because it is difficult to extract unambiguous information from featureless cross sections. Also, the cross sections will be reduced by momentum mismatch effects unless near-relativistic beam energies are used. To make any sort of analysis, the measured yield in the continuum region must be compared with some expected yield in the absence of GT strength. One possibility is to compare with the experimental background from a target nucleus having zero neutron excess. This technique was used by Goodman *et al* (1981), comparing targets of ^{42}Ca with ^{40}Ca. The nucleus ^{42}Ca has a neutron excess of two

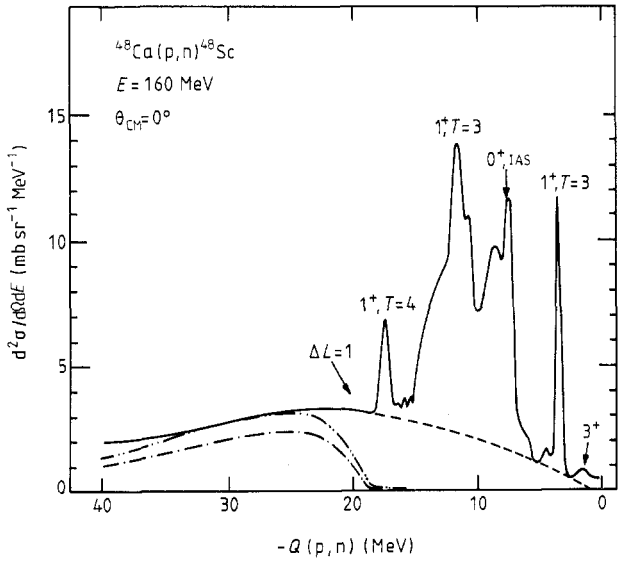

Figure 15. Zero-degree spectrum for 160 MeV (p, n) reactions on ^{48}Ca (from Osterfeld 1982). The full curve represents the experimental data. The broken curve is an arbitrary smooth background. The chain curve is the calculated background from higher multipoles ($\Delta L \geq 1$). It accounts for the experimental background at high excitations when scaled by a factor of 1.33 (— ·· —). (Used with the permission of the author and the American Institute of Physics.)

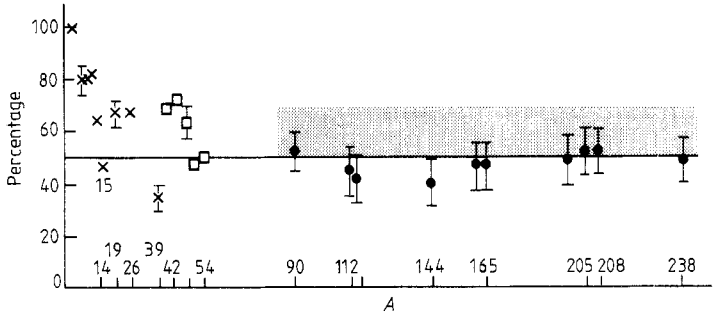

Figure 16. Fraction of the Gamow-Teller strength sum rule observed in (p, n) reactions on different targets; for heavier nuclei the full points represent the strengths concentrated in peaks, whereas the shaded region also includes the strength under the collective states (from Gaarde 1985). (Used with the permission of the author and North-Holland Publishing Company.)

with a strong GT transition to a low 1^+ state in ^{42}Ti. The strength to this state is 45% of the sum rule bound. The bound is zero in ^{40}Ca, which has equal numbers of protons and neutrons. Thus any forward-angle (p, n) cross section on this target is unrelated to a neutron excess. Goodman *et al* subtract the ^{40}Ca spectrum from the ^{42}Ca spectrum to see the effect of the neutron excess in the continuum. They find that the difference in the spectra is small above 30 MeV excitation. By identifying specific peaks, they conclude that only 50% of the sum rule is present in the spectrum. However, their plot of the difference spectrum shows a consistent excess up to 30 MeV excitation. The energy-integrated cross section in the entire region above the low peak is nearly equal to the cross section in that peak. If the excess were $L = 0$, over 80% of the sum rule bound would be present.

Analysis of the continuum region can also be made based on specific models for the background. Scholten *et al* (1983) calculated the shapes of a quasi-elastic scattering background as well as the individual low multipoles. Only the $L = 0$ multipole has a peak at forward angles. The data on ^{90}Zr in the excitation energy region of 30–50 MeV are peaked at zero degrees, so some $L = 0$ is necessary to reproduce the experiment. However, this analysis cannot be used quantitatively because it did not take into account the dependence of the interaction on the momentum transfer. A more detailed analysis was made by Klein *et al* (1985), who used the full DWIA theory. They also concluded that the continuum contained excess $L = 0$ cross section, but were unable to quantify the amount. The thorough study of Osterfeld *et al* (1985), which we discussed in § 3.3, concluded that the overall spectrum is completely consistent with the DWIA and a strength function that is only modified from the RPA by introducing additional spreading. All of these analyses assume that the DWIA is valid, i.e. multi-step reactions can be neglected. This point has been examined by Kronenfeld *et al* (1983) and Esbensen and Bertsch (1985). The multi-step reaction cross section depends strongly on beam energy; for 200 MeV protons it can contribute 5–10% to the forward-angle cross section at the GT peak.

In conclusion, we can say that at least 60% of the GT strength can be identified in the spectral range from low excitation energy to the giant GT peak. There could well be additional strength in the continuum above that, but a convincing demonstration does not seem possible with presently available experimental tools.

6.2. Theoretical discussion: subnuclear degrees of freedom

Much interest is engendered by the missing-strength question because of the implications for mesonic and other subnuclear degrees of freedom in nuclear structure. Ericson *et al* (1973) first made the suggestion that mesonic effects would suppress the GT strength. The argument was made concrete by Rho (1974), who identified the delta isobar excited state of the nucleon as the mediator of the subnucleonic influences on the spin-isospin response. The delta affects the strength in the nuclear structure domain in the same way as the higher-energy particle-hole configurations modify the low-energy transitions, taking strength away from them. In fact, the delta influence can be calculated with the identical RPA formalism, just introducing extra delta-hole states built from delta single-particle wavefunctions. The magnitude of the effects are of course crucially dependent on the nucleon-delta (NΔ) interaction. A schematic picture of the independent particle strength function including delta-hole excitations is shown in figure 17.

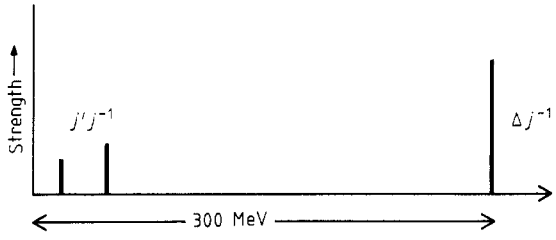

Figure 17. A schematic picture of the Gamow-Teller strength function, including the delta-hole excitations in the spectrum. The overall strength in the delta region is higher because there are no Pauli restrictions on the excited nucleons. Depending on the coupling to the states in the spectroscopic region, the residual interaction may shift substantial strength out of the low states.

Unfortunately, only the pionic part of the interaction is known with any confidence, so conclusions about the delta effects are subject to considerable uncertainty. The long-range pionic interaction is known from the $\Delta \rightarrow N\pi$ decay and can also be related to the $N \rightarrow N\pi$ interaction by the constituent quark model. A model can be built for the rest of the force by assuming that all parts of the interaction scale to the NN interaction in the same way as the pionic component. This is 'universality'. The universality argument was important in the question about the existence of a pion condensed phase of nuclear matter; for a general review see Oset *et al* (1982) or Meyer-ter-Vehn (1981). Hamiltonian models having only a pionic coupling of deltas predicted a phase transition to a different state of nuclear matter, the so-called pion condensate, contrary to empirical evidence. Models containing a repulsive component obtained from universality gave no phase transition under experimentally realisable conditions. It is this repulsive component that would be responsible for the suppression of the GT strength in the low-energy nuclear spectrum. A schematic model showing how the suppression works under universality was constructed by Bohr and Mottelson (1981). Arguing phenomenologically they arrive first at the empirical NN isospin-spin interaction, and then show that universality implies that 25% of the strength is lost from the low-energy spectrum by the coupling to the delta.

More recently, the universality assumption has been severely criticised. Arima *et al* (1983) constructed a microscopic model of the NΔ interaction based on π and ρ

meson exchanges. The exchange term provides the repulsive component of the interaction at small momentum transfers. They find that the exchange term behaves quite differently than in the NN interaction because the delta has different quantum numbers. The result is a substantially weaker repulsion, and the quenching from the delta amounts to only a few per cent. This result has been confirmed in a microscopic G matrix calculation by Sagawa *et al* (1986). Thus the theoretical argument for delta quenching is less persuasive.

Before turning to more prosaic explanations of the quenching, we mention another subnucleonic interpretation. Rho (1984) has recently put forth a radical view of the quenching, motivated by fundamental symmetry ideas. The Lagrangian of quantum chromodynamics has a near symmetry, chirality, that can be exhibited either by having massless quarks as free particles or by having massless pions. Rho speculates that pionic degrees of freedom are suppressed in nuclei. The interior of a nucleus would be more like a Fermi gas of quarks than a collection of physical nucleons. In this limit the Adler sum rule has no pion contributions and it reduces to the trivial

$$\sum_{f\mu} |\langle f|\beta^-_{\text{quark}}|i\rangle|^2 = 3(N-Z). \tag{6.1}$$

We remember that the nucleon axial coupling constant for the non-relativistic GT operator has to be modified by the pions (see equation (5.9)), so the new relation is

$$\sum_{f\mu} |\langle f|\beta^-_{\mu}|i\rangle|^2 = 3(N-Z)/g_A^2. \tag{6.2}$$

If this reasoning were correct, not only would the nuclear structure transitions be quenched by the factor $1/g_A^2 = 0.63$, but the entire strength function at delta excitation energies would disappear. In principle this speculation could be tested by neutrino-induced reactions. However, there is abundant evidence that deltas do not disappear in the nucleus. Some of it will be presented in the last section.

6.3. Theoretical discussion: configuration mixing

It is possible to explain the quenching of the spectroscopic GT strength without invoking any subnuclear degrees of freedom at all, as we saw with the analysis of Osterfeld *et al* (1985). The RPA theory and the shell model calculations we discussed in § 5 neglect configurations involving higher shells. These may take strength away from the lower energies if the interaction is strong enough. This possibility is easiest to study theoretically in nuclei with a very simple structure, as close to closed major shells as possible. This was done by Shimizu *et al* (1974), who calculated the spin properties of light nuclei removed by one nucleon from shell closure: $A = 15$, 17, 39 and 41. Including in their configuration space all states that could be reached by exciting two particles to higher shells, they found that the non-central interaction removes about 25% of the strength to high excitations.

Later studies incorporating both configuration mixing and delta excitations were made by Oset and Rho (1979) and Towner and Khanna (1979). The first work assumed universality and a limited configuration space for the configuration mixing. They concluded that the delta mechanism was the more important. Towner and Khanna, on the other hand, using a large configuration space and a microscopic treatment of the NΔ interaction, came to the opposite conclusion.

A more phenomenological argument has been made by Brown and Wildenthal (1985). They fit the effective spin operators in the spectroscopy of sd-shell nuclei and

find that the isoscalar and isovector spin operators are quenched by similar amounts. The isospin of the delta prevents it from affecting the isoscalar operator, leaving the configuration mixing as the most important influence. It is plausible to attribute a similar quenching to that source for the isovector spin operator as well. According to Brown and Wildenthal, the comparison of the quenching in the two cases suggests that the configuration mixing and the delta isobar mixing have comparable importance.

These studies concentrated on the depletion of strength in the low-energy transitions, but did not examine in detail the distribution of strength to be expected at high excitations. This aspect was studied by Bertsch and Hamamoto (1982) and Takayanagi *et al* (1985), who calculated the configuration-mixing effects on the intermediate-energy strength in the (p, n) reaction on ^{48}Ca. They found that substantial strength could be expected in the energy region of 10–40 MeV excitations. The ordinary interaction fragments the giant GT state over an approximately 10 MeV wide interval. Other microscopic studies of the fragmentation of the giant GT state also show that it gets a tail extending to high energies. At very high energies, the tensor interaction is most effective at configuration mixing.

A simple argument to show that GT strength should extend to high excitations in the continuum was made by Ericson (1983). Using a phenomenological relation between the axial field and the pion field, she expresses the GT strength in terms of the absorptive optical potential for pions. The empirical pion optical potential gives a large amount of strength in the continuum. However, the part associated with the neutron excess is only 3% of the sum rule bound.

The picture that emerges is configuration mixing transferring about 25% of the strength to the continuum. Part of this is relatively low in energy, just above the GT giant resonance, but there is also a tail that tapers off rather slowly and extends up to energies of the order of the pion rest energy.

6.4. Other charge exchange probes

We conclude this review with a discussion of some reactions which have proved helpful in elucidating the charge exchange response, besides the differential cross section in (p, n) reactions. Recently spin transfers have been measured in the (p, n) reaction, which is very interesting because of the specific dependence on the spin response. Other kinds of projectiles also have been employed in studying the charge exchange response. We shall briefly mention the (^{3}He, t) reaction, the (t, ^{3}He) reaction and the (n, p) reaction.

6.4.1. Spin measurements in (p, n). If only the differential cross section in a reaction is measured, the inferences about the spin response are heavily dependent on the theory of the response. More direct proof that the GT peak is correctly identified requires measuring the spin transferred to the target. Only the projectile spin is directly measurable, but in forward-angle scattering the projectile and target spins can only be flipped simultaneously. The forward-angle spin transfer measurement was performed recently by Taddeucci *et al* (1986) using a ^{90}Zr target. In this experiment the incoming proton is polarised transverse to the beam direction. The polarisation of the neutron is measured for orientations parallel and antiparallel to the proton spin. The observable is conveniently expressed as the transverse spin polarisation transfer coefficient D_{NN}, the ratio of the polarisation of the outgoing particle and the incoming particle. In terms of the cross sections $\sigma_{ss'}$ for incoming polarisation s and outgoing polarisation

s', D_{NN} is given by

$$D_{NN} = \frac{\sigma_{++} - \sigma_{+-}}{\sigma_{++} + \sigma_{+-}}. \tag{6.3}$$

Obviously, if the reaction is independent of spin, $\sigma_{+-} = 0$ and $D_{NN} = 1$. Of the spin-dependent amplitudes, σ_K and σ_N flip the spin, while σ_P leaves it alone. Thus if all three components of $\boldsymbol{\sigma}$ have equal amplitudes, D_{NN} will be given by $D_{NN} = (1-2)/(1+2) = -\frac{1}{3}$.

The spin measurements of D_{NN} for forward scattering give gratifying confirmation of the previous interpretation of the $L = 0$ peaks. In the region of the GT resonance the experiment found $D_{NN} = -0.29 \pm 0.03$, close to the value $-\frac{1}{3}$ expected for pure GT transitions. This result bears on the background question: if there were a background of spin-independent transitions in the GT region, it would dilute the spin flip and give a larger D_{NN}. The IAS state shows a positive D_{NN} which, however, does not reach the theoretical value of 1. In this case the conditions of the experiment do not allow a complete separation of the IAS from its background. The IAS is embedded in the tail of the GT resonance, and some of the cross section in the region has a spin flip character.

6.4.2. The (^{3}He, t) and (t, ^{3}He) reactions. As a spectroscopic tool, the (p, n) reaction suffers from the difficulty of measuring neutron energies accurately. The reaction (^{3}He, t) also changes a proton into a neutron and can be measured with good energy resolution, since the projectile and ejectile are both charged. This reaction has two disadvantages compared with (p, n). Because of the strong absorption of a complex projectile, it is not sensitive to the interior of the target. Also, an absolute theoretical determination of cross sections is more problematic due to the structural complication of the projectile. The spectroscopic characteristics of the reaction should be most comparable with the (p, n) reaction at the same velocity of the projectile and the same momentum transfer. Experiments by Gaarde *et al* (1980) showed that even with a beam energy of 70 MeV, i.e. 23 MeV (nucleon)$^{-1}$, the reaction is capable of showing the GT resonance.

Unique information has recently been obtained from the (^{3}He, t) reaction using a beam energy of 2 GeV (Contardo *et al* 1986). The high beam energy permits excitations of the nucleus into the delta region, $E_x \sim 300$ MeV. At this excitation energy the longitudinal momentum transfer (which is always greater than the energy transfer divided by c) is very high on the scale of nuclear structure studies. The response has no trace of the GT resonance physics, but in principle the experiment provides information on the dynamics of the Δ inside the nucleus. The results of this experiment show the Δ clearly and are very interesting. Figure 18 displays the spectra of tritons at zero degrees, comparing a hydrogen target with various nuclear targets. The hydrogen target can serve as a normalisation since the complexities of the projectile response will be the same for this as for the other systems. The measured spectrum shows a peak in the region of the Δ, whose energy and width correspond well to the properties of the free Δ. The interesting findings, which are easily visible in figure 18, are that the peak is also present in nuclear targets, while it has shifted about 50 MeV to a lower energy.

In a theoretical study of this reaction by Esbensen and Lee (1985), it was found that the shape and absolute magnitude of the peak in hydrogen could be understood quantitatively by assuming that the spin response of the mass-3 projectile depends on momentum in the same way as the point-particle charge form factor. The correct

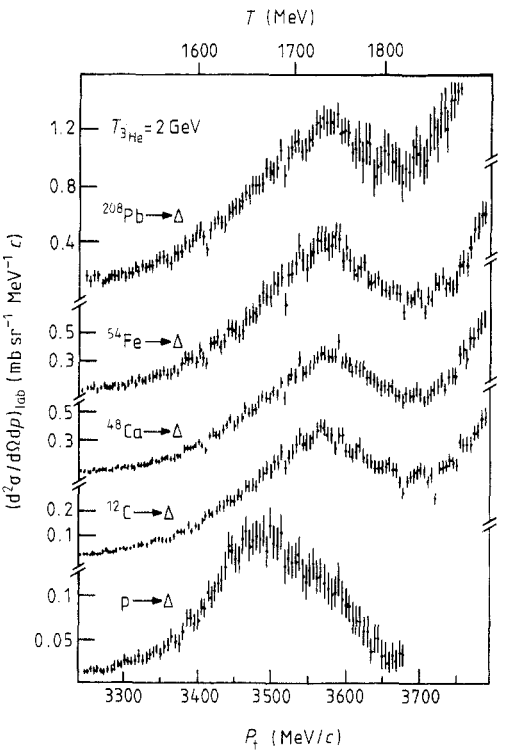

Figure 18. Triton spectra observed in 2 GeV (^{3}He, t) reactions on hydrogen and on different nuclear targets at zero degrees; notice the shift of the peak position to a 50 MeV smaller excitation energy for reactions on the nuclear targets (from Contardo *et al* 1986). (Used with the permission of the authors and North-Holland Publishing Company.)

orders of magnitude of the nuclear target cross section as well as the observed peak position are reproduced when an empirically adjusted self-energy of the Δ in a nuclear medium is used. The (^{3}He, t) reaction takes place at the surface of the target nucleus, and one might suspect that a microscopically calculated, density-dependent self-energy could yield a different result and destroy the agreement with the data. Future studies will hopefully resolve this problem.

We also mention here the inverse reaction (t, ^{3}He). This would provide potentially valuable information on the β^+ strength function, as discussed below. Unfortunately, the highest-energy tritium beam available is 25 MeV, which allows only minimal spectroscopic information to be extracted. Nevertheless, the reaction has been used to identify states with appropriate spin for GT transitions and to measure relative cross sections (Ajzenberg-Selove *et al* 1984).

6.4.3. The (n, p) reaction. As discussed in § 5, the β^+ operator has quite different structural characteristics from the β^- operator in nuclei with neutron excess. The residual interaction in the nuclear Hamiltonian tends to correlate all the protons with neutrons so that the β^+ strength is nearly completely suppressed. The amount of strength left provides a good test of the Hamiltonian model; the (n, p) reaction cross section is additionally sensitive to Δ admixtures (Brown and Wildenthal 1983). Experimentally the (n, p) reaction is very difficult to measure, and to date the only spectroscopic application in the literature is the experiment by Brady *et al* (1983) using 60 MeV

neutrons on a target of ^{7}Li. In this work it was found that the $L = 0$ strength is weak; in fact the most prominent feature of the spectrum is an $L = 1$ peak at higher energy. For more quantitative measurements of the β^+ response it is of course necessary to use higher-energy projectiles. Recently, an (n, p) facility has been constructed at the TRIUMF laboratory in Vancouver that can produce neutron beams extending in energy to hundreds of MeV. A preliminary spectrum of a ^{54}Fe target is shown in figure 19 (from Häusser *et al* 1986). There is a prominent peak at low excitation energy, showing a substantial concentration of β^+ strength. With this new capability for (n, p) studies, it should be possible to answer the questions still remaining about the β^+ strength.

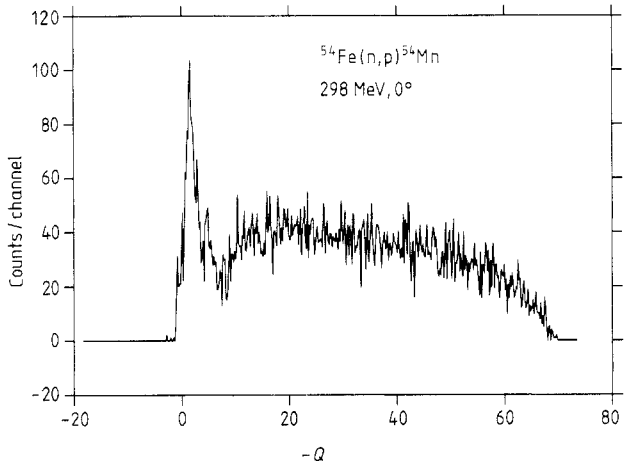

Figure 19. The proton spectrum observed in 300 MeV (n, p) reactions on ^{54}Fe at zero-degree scattering. Note the strength concentration at very low excitation energies (from Häusser *et al* 1986). (Used with the permission of the authors prior to publication.)

Acknowledgments

We are grateful to B A Brown, C Gaarde, D Kurath, T-S H Lee, H Lipkin, K Nakayama and R Wiringa for discussions and advice on various parts of this manuscript. GFB is supported in part by the National Science Foundation under Grant PHY85-19653. HE is supported by the US Department of Energy, Nuclear Physics Division, under contract W-31-109-ENG-38.

References

Abrikosov A A and Khalatnikov I M 1959 *Rep. Prog. Phys.* **22** 329
Adler S L and Dashen R F 1968 *Current Algebras* (New York: Benjamin)
Ajzenberg-Selove F, Brown R E, Flynn E R and Sunier J W 1984 *Phys. Rev.* C **30** 1850
Alford W P *et al* 1986 *Phys. Lett.* **179B** 20
Anderson J D and Wong C 1961 *Phys. Rev. Lett.* **7** 250
Anderson J D, Wong C and Madsen V A 1970 *Phys. Rev. Lett.* **24** 1074
Arima A, Cheon T, Shimizu K, Hyuga H and Suzuki T 1983 *Phys. Lett.* **122B** 126
Arndt R A, Roper L D, Bryan R A, Clark R B, VerWest B J and Signell P 1983 *Phys. Rev.* D **28** 97

Auerbach N, Zamick L and Klein A 1982 *Phys. Lett.* **118B** 256
Austin S M 1980 *The (p, n) Reaction and the Nucleon-Nucleon Force* ed C D Goodman *et al* (New York: Plenum) p 203
Babu S and Brown G E 1973 *Ann. Phys., NY* **78** 1
Bäckmann S O, Sjöberg O and Jackson A D 1979 *Nucl. Phys.* A **321** 10
Bainum D E, Rapaport J, Goodman C D, Horen D J, Foster C C, Greenfield M B and Goulding C A 1980 *Phys. Rev. Lett.* **44** 1751
Bertsch G F 1983 *Prog. Theor. Phys., Suppl. No* **74/75** 115
Bertsch G F, Borysowicz J, MacManus H and Love W G 1977 *Nucl. Phys.* A **284** 399
Bertsch G F, Cha D and Toki H 1981 *Phys. Rev.* C **24** 533
Bertsch G F and Hamamoto I 1982 *Phys. Rev.* C **26** 1323
Bethe H A 1971 *Ann. Rev. Nucl. Sci.* **21** 93
Bethe H A, Brown G E, Applegate J, and Latimer J N 1979 *Nucl. Phys.* A **324** 487
Blair J S 1959 *Phys. Rev.* **115** 928
Bloom S D and Fuller G M 1985 *Nucl. Phys.* A **440** 511
Bohr A and Mottelson B R 1981 *Phys. Lett.* **100B** 10
Brady F, Needham G A, Romero J L, Castaneda C M, Ford T D, Ullmann J L and Webb M L 1983 *Phys. Rev. Lett.* **51** 1320
Brieva F A and Rook J R 1978 *Nucl. Phys.* A **297** 206
Brown B A, Chung W and Wildenthal B H 1981 *Bull. Am. Phys. Soc.* **26** 1144
Brown B A and Wildenthal B H 1983 *Phys. Rev.* C **28** 2397
—— 1985 *At. Data Nucl. Data Tables* **33** 347
Carey T A, Jones K W, McClelland J B, Moss J M, Rees L B, Tanaka N and Bacher A D 1984 *Phys. Rev. Lett.* **53** 144
Cha D 1983 *Phys. Rev.* C **27** 2269
Clark B C, Hama S, Mercer R L, Ray L and Serot B D 1983 *Phys. Rev. Lett.* **50** 1644
Cohen S and Kurath D 1965 *Nucl. Phys.* **73** 1
Contardo D *et al* 1986 *Phys. Lett.* **168B** 331
Day B D 1967 *Rev. Mod Phys.* **39** 719
—— 1981 *Phys. Rev.* C **24** 1203
Dickhoff W H 1983 *Nucl. Phys.* A **399** 287
Dickhoff W H, Faessler A, Muther H and Wu S-S 1983 *Nucl. Phys.* A **405** 534
Doering R R, Galonsky A, Patterson D M and Bertsch G F 1975 *Phys. Rev. Lett.* **35** 1691
Ericson M 1983 *Phys. Lett.* **120B** 285
Ericson M, Figureau A and Thevenet D 1973 *Phys. Lett.* **45B** 19
Esbensen H and Bertsch G F 1985 *Phys. Rev.* C **32** 553
Esbensen H and Lee T-S H 1985 *Phys. Rev.* C **32** 1966
Gaarde C 1983 *Nucl. Phys.* A **396** 127c
—— 1985 *Nuclear Structure* ed R Broglia *et al* (Amsterdam: Elsevier) p 449
Gaarde C, Larsen J S, Harakeh M N, Van Der Werf S V, Igaashi M and Muller-Arnke A 1980 *Nucl. Phys.* A **334** 248
Gaarde C, Rapaport J, Taddeucci T N, Goodman C D, Foster C C, Bainum D E, Goulding C A, Greenfield M B, Horen D J and Sugarbaker E 1981 *Nucl. Phys.* A **369** 258
Goodman C D and Bloom S D 1984 *Spin Excitations in Nuclei* ed F Petrovich *et al* (New York: Plenum) p 143
Goodman C D, Goulding C A, Greenfield M B, Rapaport J, Bainum D E, Foster C C, Love W G and Petrovich F 1980 *Phys. Rev. Lett.* **44** 1755
Goodman C D *et al* 1981 *Phys. Lett.* **107B** 406
Hamada T and Johnston I D 1962 *Nucl. Phys.* **34** 382
Häusser O *et al* 1986 to be published
Haybron R M and MacManus H 1964 *Phys. Rev.* **136B** 1730
—— 1965 *Phys. Rev.* **140B** 638
Holinde K, Erkelenz K and Alzetta R 1972 *Nucl. Phys.* A **198** 598
Horen D J *et al* 1981 *Phys. Lett.* **99B** 383
Ikeda K, Fujii S and Fijita J I 1963 *Phys. Lett.* **3** 271
Jeukenne J P, Lejeune A and Mahaux C 1976 *Phys. Rep.* **25** 83
Kazarinov Yu and Simonov Yu N 1963 *Sov. Phys.-JETP* **16** 24
Kerman A K, MacManus H and Thaler R M 1959 *Ann. Phys., NY* **8** 551
Kisslinger L and Sorensen R 1963 *Rev. Mod. Phys.* **35** 853
Klapdor H 1981 *Z. Phys.* A **299** 213

Klein A, Love W G and Auerback N 1985 *Phys. Rev.* C **31** 710
Kobas A M, Mackintosh R S and Rook J R 1982 *Nucl. Phys.* A **389** 205
Kronenfeld J, Gal A and Eisenberg J M 1983 *Nucl. Phys.* A **402** 569
Lacombe M, Loiseau B, Richard J M, Vinh Mau R, Cote J, Pires P and de Tourreuil R 1980 *Phys. Rev.* C **21** 861
Love W G and Franey M A 1981 *Phys. Rev.* C **24** 1073
—— 1983 *Phys. Rev.* C **27** 438E
—— 1985 *Phys. Rev.* C **31** 488
Love W G, Franey M A and Petrovich F 1984 *Spin Excitations in Nuclei* ed F Petrovich *et al* (New York: Plenum) p 205
MacGregor M H *et al* 1960 *Ann. Rev. Nucl. Sci.* **10** 291
McNeil J A, Ray L and Wallace S J 1983 *Phys. Rev.* C **27** 2123
Madey R *et al* 1987 *Phys. Rev.* C in press
Meyer H O and Schwandt P 1981 *Phys. Lett.* **107B** 353
Meyer H O, Schwandt P, Moake G L and Singh P P 1981 *Phys. Rev.* C **23** 616
—— 1983 *Phys. Rev.* C **27** 459
Meyer-ter-Vehn J 1981 *Phys. Rep.* **74** 323
Muto K 1986 *Nucl. Phys.* A **451** 481
Nadasen A, Schwandt P, Singh P P, Jacobs W W, Bacher A D, Debevac P T, Kaitchuck M D and Meek J T 1981 *Phys. Rev.* C **23** 1023
Nakayama K 1985 *Thesis* University of Bonn
Nakayama K, Galeao A P and Krmpotic F 1982 *Phys. Lett.* **114B** 217
Nakayama K, Krewald S, Speth J and Love W G 1984 *Nucl. Phys.* A **431** 419
Nanda S K *et al* 1983 *Phys. Rev. Lett.* **51** 1526
Negele J W and Vautherin D 1972 *Phys. Rev.* C **5** 1472
Nolen J A and Schiffer J P 1969 *Ann. Rev. Nucl. Sci.* **19** 471
Oset E and Rho M 1979 *Phys. Rev. Lett.* **42** 47
Oset E, Toki H and Weise W 1982 *Phys. Rep.* **83** 281
Osterfeld F 1982 *Phys. Rev.* C **26** 762
Osterfeld F, Cha D and Speth J 1985 *Phys. Rev.* C **31** 372
Petrovich F, McManus H, Madsen V A and Atkinson J 1969 *Phys. Rev. Lett.* **22** 895
Rapaport J, Kulkarni V and Finlay R 1979 *Nucl. Phys.* A **330** 15
Raynal J 1967 *Nucl. Phys.* A **97** 572
Reid R V 1968 *Ann. Phys., NY* **50** 411
Rho M 1974 *Nucl. Phys.* A **231** 493
—— 1984 *Ann. Rev. Nucl. Part. Sci.* **34** 531
Sagawa H, Lee T-S H and Ohta K 1986 *Phys. Rev.* C **33** 629
Sagawa H and Van Gai N 1982 *Phys. Lett.* **113B** 119
Satchler G R 1983 *Nucl. Phys.* A **394** 349
Scholten O, Bertsch G F and Toki H 1983 *Phys. Rev.* C **27** 2975
Shimizu K, Ichimura M and Arima A 1974 *Nucl. Phys.* A **226** 282
Speth J 1980 *Nucl. Phys.* A **343** 382
Stapp H P, Ypsilantis T J and Metropolis N 1957 *Phys. Rev.* **105** 302
Sterrenburg W A, Austin S M, DeVito R P and Galonsky A 1980 *Phys. Rev. Lett.* **45** 1839
Taddeucci T N *et al* 1986 *Phys. Rev.* C **33** 746
Takayanagi K, Shimizu K and Arima A 1985 *Nucl. Phys.* A **444** 436
Tjon J A and Wallace S J 1985a *Phys. Rev.* C **32** 267
—— 1985b *Phys. Rev. Lett.* **54** 1357
Towner I S and Khanna F C 1979 *Phys. Rev. Lett.* **42** 51
Watson J W, Pairsuwan W, Anderson B D, Baldwin A R, Flanders B S, Madey R, McCarthy R J, Brown B A, Wildenthal B H and Foster R C 1985 *Phys. Rev. Lett.* **55** 1369
Wildenthal B H 1984 *Prog. Part. Nucl. Phys.* **11** 5
Wolfenstein L and Ashkin J 1952 *Phys. Rev.* **85** 947
Zamick L 1966 *Phys. Lett.* **21** 194